ABSTRACT

Title of Thesis:	Expression and Purification of the Cell-Penetrating Peptide MAP Fused to Protein Cargo
	Ren-Jhe Chung, Master of Science, 2024
Thesis Directed By:	Prof. Amy J. Karlsson Department of Chemical and Biomolecular Engineering

Candida albicans is a common fungal pathogen that presents a significant public health issue due to its resistance to traditional antifungal small molecule medications. While large therapeutics offer potential as alternative treatments with novel mechanisms of action, their efficacy is hindered by low cellular uptake and limited accessibility to intracellular targets. Cell-penetrating peptides (CPPs) are promising vehicles for facilitating the intracellular delivery of large biomolecules. CPPs are short protein peptides capable of crossing various membrane barriers, even when conjugated to cargo molecules. However, producing CPP fusion proteins can be challenging due to their higher toxicity to host cells. To enhance expression, we studied and optimized several contributing factors, including expression partners, host cell strains, sequential order of CPP and cargo, and induction conditions, for the fusion of CPP MAP to the cargo monomeric enhanced green fluorescent protein (meGFP). Our findings indicated that the expression partner, combined with positioning MAP at the N-terminus of the cargo, resulted in relatively high expression levels.

The highest expression level was achieved in the BL21(DE3) *Escherichia coli* strain, with induction at 20°C for 24 hours. These results support further research on the application of MAP recombinant proteins and lay the foundation for the generalization of CPP recombinant protein expression.

Expression and Purification of the Cell-Penetrating Peptide MAP Fused to Protein Cargo

by

Ren-Jhe, Chung

Thesis submitted to the Faculty of the Graduate School of the
University of Maryland, College Park, in partial fulfillment
of the requirements for the degree of
Master of Science
2024

Advisory Committee:
Professor Amy J. Karlsson
Professor Ganesh Sriram
Professor Peter Kofinas

Dedication

This thesis is dedicated to my beloved parents, Sheng-Wei Chung and Yun-Min Ko, and my family for their endless support and encouragement throughout my master's path.

Acknowledgements

I would like to express my deepest appreciation to everyone who has supported, guided, and inspired me throughout my academic journey in completing this thesis.

First and foremost, I want to thank my advisor, Dr. Amy Karlsson, for her continuous support and guidance throughout my master's degree. It was her invaluable advice, patience, and encouragement that helped me overcome the most challenging moments of my graduate studies. I can never thank her enough for the strength and courage she has instilled in me to tackle any obstacle.

I am also profoundly thankful to my labmates, Dr. Wright Makambi and Dr. Dinara Konakbayeva, for their constant support, collaboration, and training. I can barely imagine completing the master's thesis without their help. Their willingness to share their knowledge and provide assistance has been crucial to my progress, and I truly appreciate the friendship we have built.

Additionally, I would like to acknowledge our previous lab members, Marzyeh Kheradmand-Hajibashi, and Dr. Shakiba Nikfarjam. Thank you for helping me build my lab skill set and giving me insights into my work.

Finally, I would like to thank my family and friends for their unwavering support and understanding throughout this journey. Their encouragement has been a source of strength and motivation.

Thank you all for being an integral part of this endeavor.

Table of Contents

List of Tables

List of Figures

List of Abbreviations

CFPS	Cell-free protein synthesis
CPP	Cell-penetrating peptides
DI water	Deionized water
DMD	Duchenne muscular dystrophy
DNA	Deoxyribonucleic acid
DTT	Dithiothreitol
Factor Xa	Activated enzyme for Factor X
FDA	Food and Drug Administration
GFP	Green fluorescent protein
GST	Glutathione S-transferase
G_4S	Glycine-serine
HRP	Horseradish peroxidase
IMAC	Immobilized metal affinity chromatography
IPTG	β-d-1-thiogalactopyranoside
LB	Luria Bertani
MBP	Maltose-binding protein
meGFP	Monomeric enhanced green fluorescent protein
NaPB	Sodium phosphate
PCR	Polymerase chain reaction
PVDF	Polyvinyl difluoride
RNA	Ribonucleic acid
RPM	Round per minute
SEC	Size exclusion chromatography

SDS-PAGE	Sodium dodecyl sulfate polyacrylamide gel electrophoresis
SDS	Sodium dodecyl sulfate
SOC	Super optimal broth with catabolite
T7 tag	Bacteriophage T7 epitope tag
6x His	Hexahistidine

Chapter 1: Introduction

1.1 Candida albicans, relating diseases and treatment

1.1.1 *Candida* species emergency in public health

Candida species are among the most widespread fungal pathogens causing global health issues due to limited research and data on fungus infection, drug resistance, and public health impact. This pathogen can easily survive and grow under non-extreme conditions, including the human body. *Candida* species usually live in mucosal areas, such as the vagina, mouth, throat, or esophagus, as part of the microbiome in the human body without causing any problems to their hosts' health. However, if the living microenvironment favors *Candida* species growth or the immune ability of the host is weakened, its growth may become out of control and lead to a fungal infection, which is also known as candidiasis, with the symptoms including itching, soreness, redness, in infection area and fever and chills [1]. The symptoms can be even more severe and life-threatening if the infection has developed in the brain, heart, or other life-sustaining organs, also known as systemic *Candida* infection or invasive candidiasis. The lethality of bloodstream-invasive *Candida* infection is up to 25% [1], which can be even higher for immunocompromised and post-operative patients [1].

1.1.2 *Candida albicans*

Among all the *Candida* species, *Candida albicans* is the most common one. *C. albicans* has two different forms directly related to its virulence and survival. Generally, *C.*

albicans in yeast form is more susceptible to stress and thus less likely to lead to fungal infection. However, *C. albicans* can rapidly change from yeast to hyphal forms through filamentation under growth conditions at pH 7 and 37°C. The hyphae of *C. albicans* can interact with hypha filamented from other *C. albicans* cells (Figure 1.1), thus building up a tensely cross-linked biofilm that protects it from environmental stress [12]. Although *C. albicans* is naturally present in the human body, the hyphal form of *C. albicans* and its resulting protective biofilm can break the microbiome balance in the human body and make it more resilient against antifungal medication.

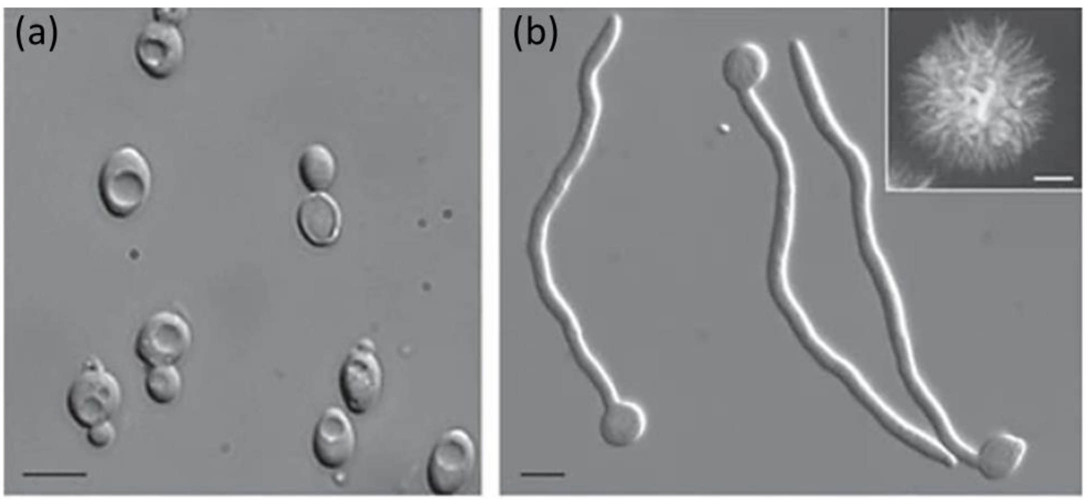

Figure 1.1. The yeast form (a) and the hyphal form (b) of *C. albicans*. The scale in the figure represents 5 μm. Figure reprinted with permission from Sudbery et al. [12]. Copyright 2004 Elsevier Ltd 46.

1.1.3 Traditional treatment for *Candida* infection

Azoles, echinocandins, and polyenes are the primary classes of traditional treatment against fungal infections (Figure 1.2). Fluconazole is an FDA-approved drug that belongs to the tri-azole family, one of the most widely used antifungal medications that can treat both mucosal and systemic *Candida* infections. Fluconazole interacts with 14-demethylase, a critical enzyme for the formation of ergosterol from lanosterol, Since ergosterol is of vital essence in fungal plasma membrane, the membrane permeability of *Candida* cells significantly increases after the introduction of fluconazole. Endogenous respiration and cell growth are also impaired by fluconazole [2]. Echinocandin drugs block the synthesis of β-(1,3)-D-glucan, a critical glycoprotein in the fungal cell wall, by binding to the FKS1/2 subunit of the glycosyltransferase, responsible for glucan production. The binding can greatly decrease the bioactivity of the glycosyltransferase, leading to low production of β-(1,3)-D-glucan. Without the presence of β-(1,3)-D-glucan, the fungal cell walls are highly unstable, resulting in growth inhibition and cell death. Since β-(1,3)-D-glucan is not present in mammalian cells, echinocandin drugs are widely used for treating severe fungal infections [3]. Amphotericin B, a member of the polyene class drug, is commonly used as a primary antifungal medication. The hydrophobic part of amphotericin B can bind to ergosterol and open pores and channels on the membrane that allow material to exchange rapidly between the intracellular and extracellular environments. This results in osmotic disturbance in the fungal cell membrane and causes cell death [13].

Table 1.1. The chemical structure of representative traditional antifungal molecular drugs. Figure reprinted with permission from PubChem Compound Summary [58,59,60]. Copyright 2024 PubChem limited.

Fluconazole (azole drug)	Anidulafungin (echinocandin drug)	Amphotericin B (polyene drug)
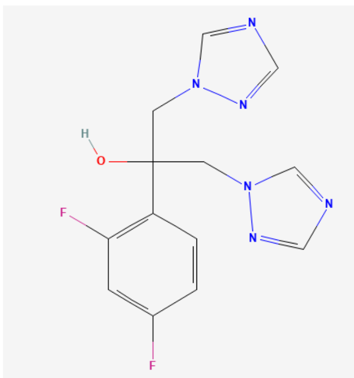	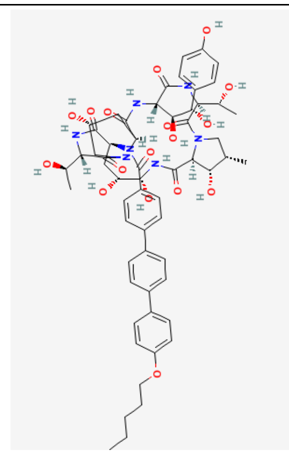	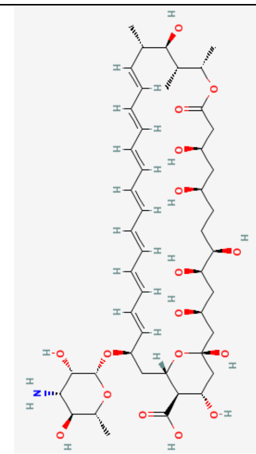

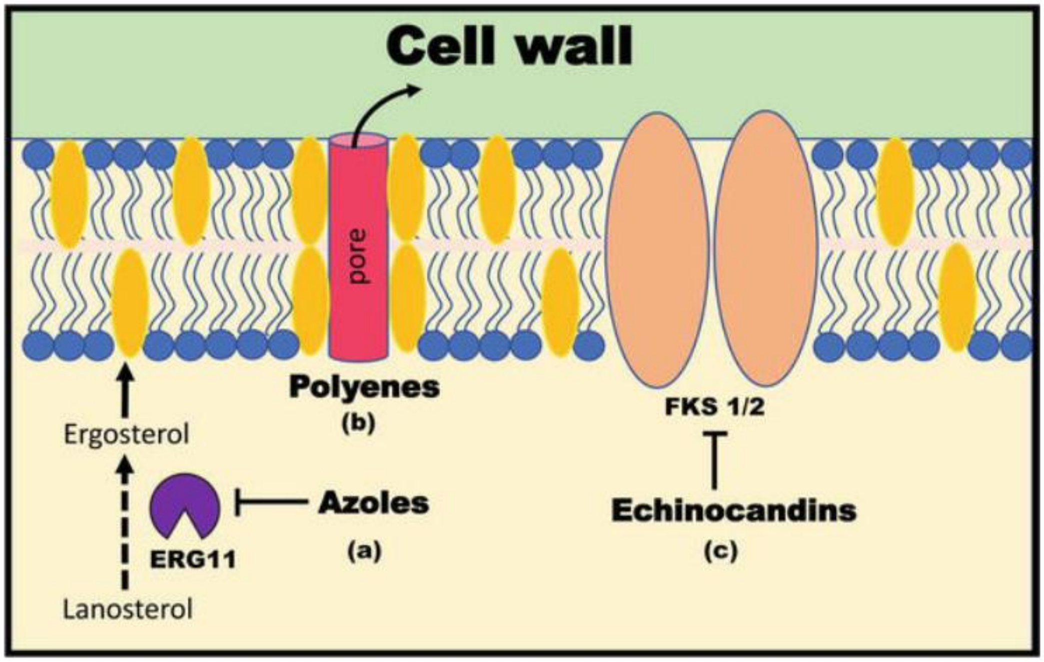

Figure 1.2. The mechanisms for traditional antifungal medications, including azole, echinocandin, and polyene drugs. Figure reprinted with permission from Ruiz-Baca et al. under the terms of the Creative Commons Attribution 3.0 License [14]. Copyright 2024 IntechOpen limited.

1.1.4 Drug resistance in *Candida* species

Currently, around 7% of all *Candida* species have developed drug resistance to fluconazole [2], and certain *Candida* species, particularly *C. glabrata* and *C. lusitaniae*, have gained resistance to echinocandins or amphotericin B [3,13]. *Candida* cells can develop resistance through various methods, including alteration of the enzyme target for the medication, overexpression of drug efflux proteins to remove the drug from the intracellular environment, reduction of ergosterol in the cell membrane, and increasing stress tolerance [14]. Patients suffering from *Candida* infections that are resistant to these three medications have few treatment options to kill this fungal pathogen. An alternative treatment other than traditional small-molecule drugs is a must to deal with this global health issue.

1.2 Cell-penetrating peptides (CPPs)

1.2.1 Introduction of cell-penetrating peptides (CPPs)

Considering the existing resistance against small molecule drugs, large therapeutics, such as proteins and nucleic acids, with new methods of action could be potential candidates to treat *Candida* infections. However, both the stability of these peptides and the corresponding cellular uptake greatly limit the potency of these therapeutics, further making it necessary to introduce high doses of therapeutics to reach medical effects with more concerns about significant side effects [46]. The process of internalizing these extracellular peptides is also challenging. An efficient delivery carrier is needed to ensure the delivery of the antifungal peptides in various cell types, even challenging ones, and the availability to reach its target.

The cell membrane is one of the most challenging parts in the drug delivery process. Due to the lipid bilayer structure, most biomolecules and therapeutics, including large ones such as proteins and lipids, cannot cross the membrane via passive diffusion driven by concentration gradient [17]. There are several approaches to increase the permeability of these large molecules, including lipids, and nanoparticles. However, most of the strategies failed to reach high translocation efficiency and the effectiveness of translocation while complexing with biomolecules.

One promising candidate for an intracellular drug delivery strategy for large molecules is cell-penetrating peptides (CPP). CPPs are short peptides composed of 5-30 amino acids. They efficiently cross various cell membrane barriers, including mammalian, bacterial, and fungal cells, via several translocation mechanisms, mainly endocytosis or direct penetration, while carrying various cargos such as DNA, proteins, or therapeutics (Figure. 1.3). The capabilities of intracellular targeting and specific translocation make CPPs ideal candidates for drug delivery carriers [4,16,17].

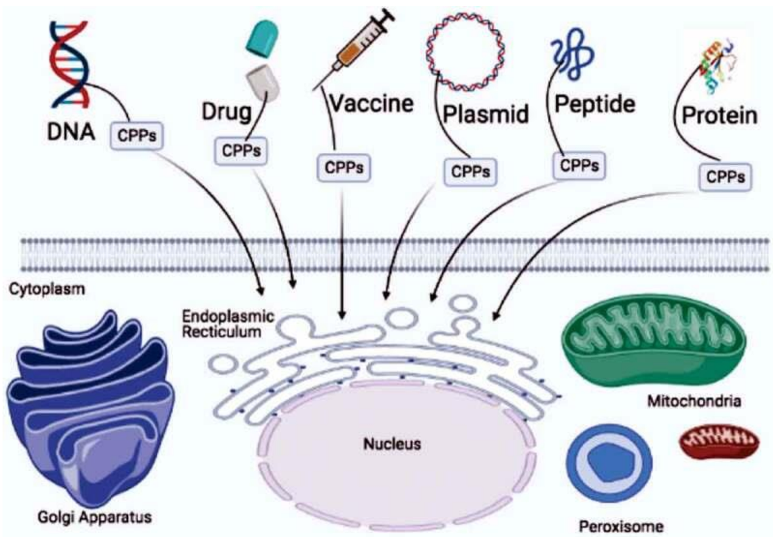

Figure 1.3. Various CPP-cargo complex designs and potential intracellular targets [16]. Figure reprinted with permission from Sadiq et al. [16]. Copyright 2024, Taylor & Francis limited.

1.2.2 Classification of CPPs

The classification of CPPs can be based on either its origin or its physicochemical properties. Based on its origin, CPPs can be classified into three main categories: chimeric synthetic and protein-derived CPPs [16]. On the other hand, CPPs can be classified as cationic, amphipathic, or hydrophobic based on their physicochemical properties [16].

Category based on peptide origin:

Chimeric CPPs: Chimeric CPPs refer to hybrid or recombinant proteins composed of two or more different motifs in various peptides to combine the characteristics of different proteins. TP10 is an example of a chimeric CPP. By linking mastoparan, a 14-residue peptide derived from wasp venom, to 6 residues from neuropeptide galanin by an additional lysine, TP10 can interact with the lipid bilayer and thus penetrate the bacterial and protozoa cell membrane [16, 18].

Synthetic CPPs: Synthetic CPPs are a given amino sequence which is not naturally presented in real world, and therefore synthetic CPPs are usually produced via chemical reactions, which allows the large-scale production of identical synthetic CPPs. Synthetic CPPs are usually discovered through rational design and combinatorial experiments to improve the existing functional peptide sequences [19]. Based on its design, synthetic CPP can be used to study protein folding, modify the structural characteristics of existing biologics, or even develop novel protein therapeutics [16, 48].

Protein-derived CPPs: Protein-derived CPPs are derived from naturally present proteins, most of which are involved in hydrolysis, fermentation, or digestion [51]. These metabolic mechanisms involve transporting biomolecules from the extracellular environment. In fact, one of the first discovered CPPs, TAT, is a protein-derived CPPs, originating from HIV-1 protein and it has the ability to penetrate mammalian cell membranes.

Category based on physiochemical property:

Cationic CPPs: A cationic CPP has lots of positively charged amino acids in its sequence, which facilitate the process of crossing the cell membrane by electrostatic interaction with the negatively charged components in the cell membrane surface, including carboxylic, sulfate, and phosphate groups, which is a critical step for the direct penetration pathway (discussed below) in CPP translocation [20]. TAT contains lots of positively charged residues in its sequence (RKKRRQRRR) to make it overall cationic. Based on the number of arginine and lysine in its sequence, the penetration effectiveness may vary [16].

Amphipathic CPPs: Amphipathic CPPs are both hydrophilic and hydrophobic, which facilitates their interaction with the hydrophobic and hydrophilic groups of the lipid bilayer in the cell membrane and thus allows them to cross the membrane barrier. Amphipathicity is a critical factor determining the membrane binding properties and translocation efficiency in both endocytosis and direct penetration pathway [16,20].

Hydrophobic CPPs: Hydrophobic peptides consist of nonpolar amino acids or hydrophobic domains, which make the peptide nearly uncharged. Hydrophobicity also plays an important role in translocation across the cell membrane via interaction with the lipid bilayer in the endocytosis pathway [16].

1.2.3 Translocation mechanisms

There are several pathways available for CPPs to enter the targeting cell based on the physiochemical properties of CPPs. The main uptake pathways are direct penetration and endocytosis [8].

Direct penetration is an energy-independent pathway, the main internalization pathway for some cationic or amphipathic CPPs. The positively charged residues will interact with the negatively charged cell membrane components, such as phospholipid and heparan sulfate. The hydrophobic and electrostatic interaction between the CPP and membrane allows CPPs to bind to the membrane and further destabilize the membrane structure, such as thinning the membrane, forming pores, or forming a micelle that can be transported into the cell (Figure 1.4) [5,8,21,26]. However, this mechanism is not as effective as endocytic mechanisms if the concentration of CPPs is low in the extracellular environment.

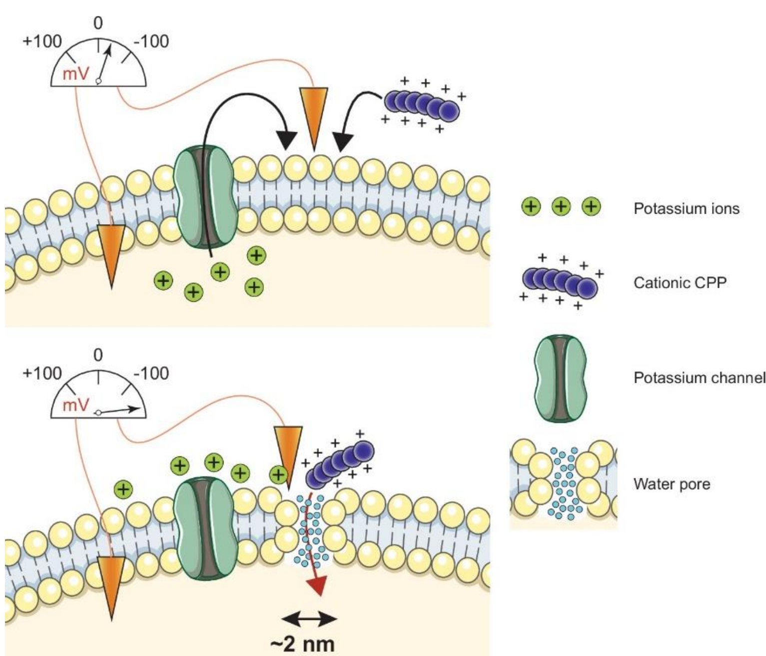

Figure 1.4. An example of direct penetration translocation for cationic CPPs. Figure reprint with permission from Trofimenko et al. [26]. Copyright Trofimenko et al, 2021 limited.

Endocytosis is an energy-dependent process for cells to naturally internalize large molecules such as proteins, lipids, and nucleic acids. Endocytosis is also responsible for maintaining cell membrane composition and signaling for both intracellular and extracellular receptors. There are several possible pathways for endocytosis, including macropinocytosis, phagocytosis, and receptor-mediated endocytosis (Figure 1.5) [5,8,16]. In macropinocytosis, the outer cell membrane bends and forms a space to recruit molecules from the extracellular environment. In the end, the bent membrane forms a large vesicle, a macropinosome, that can be transported into the cell plasma with the help of dynamin proteins such as actin [53]. Phagocytosis is an uptake pathway with high efficiency for immune cells such as macrophages, neutrophils, and dendritic cells [54]. After the phagocytic receptors detect the corresponding molecules, several signaling pathways will be activated to reorganize the actin skeleton to form a cup structure on the membrane touching the particles [6,8]. The cup will soon become a vesicle when the cell membrane seals the opening on the cup, phagosome, and then be transported into the cytoplasm. Receptor-mediated endocytosis is a cell uptake pathway involving clathrin or caveolin proteins. These proteins are covered from the interior side of the cell membrane to facilitate invagination formulation where the particles touch membranes. While the caveolin-mediated pathway can uptake molecules with a size around hundreds of nanometers, clathrin-mediated endocytosis can internalize those around 50-80 nanometers [16,55,56].

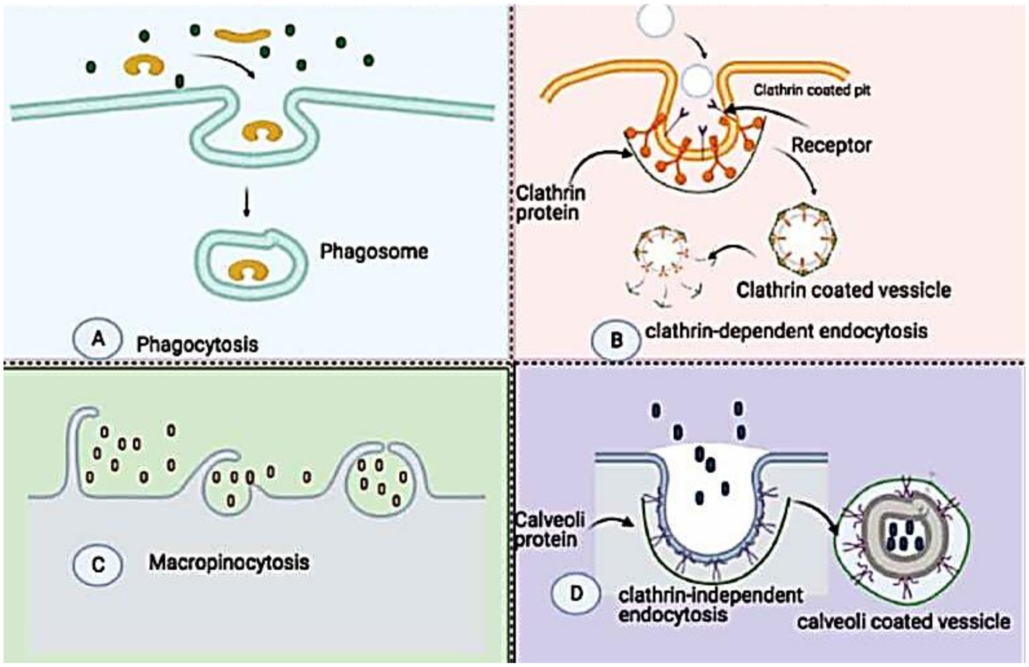

Figure 1.5 Types of endocytosis pathway [16]. (a) phagocytosis (b) clathrin-mediated endocytosis (c) macropinocytosis (d) calveoli-mediated endocytosis. Figure reprinted with permission from Sadiq et al [16]. Copyright 2024, Taylor & Francis limited.

However, the cellular uptake mechanism still remains unclear and needs further examination for most CPPs, since the testing method may lead to different results. For instance, fluorescein or another fluorescence label is often added to the CPP construct to measure the uptake of CPPs in designated cell lines, which may trigger a pathway other than the usual one to internalize non-fluorescent biomass [7,8]

1.3 Successful application of CPPs

Due to the ability to cross the cell membrane barrier, there are several successful and potential applications for CPP as a delivery vehicle for intracellular targets. Though most of the pre-clinical studies focus on CPP translocation into mammalian cells, some research also shows its application in bacterial and fungal cells.

1.3.1 Preclinical application

In fact, there are several successful applications of CPP-therapeutics complexes in preclinical studies. For traditional cancer therapy, patients use chemotherapeutics at high concentration levels to ensure the lethality of the tumor cell, which not only increases the cost of treatment but also damages healthy cells in the patient body. This can be addressed via conjugating chemotherapeutics with CPPs due to their specificities. Via conjugating chemotherapeutics with properly modified CPPs [4], the biodistribution and the pharmacokinetic profile of chemotherapy drugs can be potentially increased. Another CPP application in the medical field is the treatment of Duchenne muscular dystrophy (DMD). The cause of DMD is either mutation or deletion in the dystrophin gene, resulting in early termination in the translation of dystrophin, a protein that facilitates interaction between cytoskeletons. Deficient or partial functional dystrophin would lead to highly fragile and permeable cell membranes, in turn resulting in decreased regeneration capacity in muscle fiber. Antisense oligonucleotides are one viable approach to deal with DMD skipping of exons with mutations or deletions in the dystrophin gene. Since the oligonucleotides are only effective in intracellular environments, the conjugation of CPP, such as PMO, to antisense oligonucleotides are favorable to facilitate their delivery across the plasma membrane [4,22].

1.3.2 Bacterial application

CPPs can be used to deliver functional proteins and thereby alter the expression of specific proteins and the phenotype of the bacterial cells. This enables a plasmid-free process to regulate the protein expression and make a single cell to express different kinds of proteins depending on the functional protein delivered by CPPs. Lee et al. successfully used CPPs to deliver I-SceI restriction enzyme to remove plasmid with the corresponding recognition site in *Escherichia coli* cells [9]. This can prevent cell damage or unintended mutation that occurs in traditional plasmid removal methods, which induce mutations in the plasmid to prevent it from replicating by adding chemical reagents.

1.3.3 Fungal applications

More studies about CPPs focus on mammalian and bacterial cells, though there are reported applications of CPPs in fungal cells. CPP-conjugated antifungal drugs can be used as a promising treatment for fungal keratitis in the cornea [25]. The complexation with the CPP Tat_2 allows the small molecular drugs to cross the epithelial barrier in the cornea, which enables the same bioactivity with antifungal drugs at low concentrations. This greatly reduces the systematic toxicity of antifungal drugs due to high concentration, leading to higher biocompatibility of these drugs.

Previous research from Gong et al. shows that some CPPs previously used in other cell types, including penetratin, pVeC, MAP, SynB, $(KFF)_3K$, MPG, PAF26, and Pep-1, can be internalized by *C. albicans* [11]. In this study, the CPPs were first fused to a small molecule cargo fluorescein, a fluorescent dye could be easily detected; the result shows that CPPs with higher net charge (≥+4) have higher translocation efficiency, while those with lower to zero net charge show limited translocation in *Candida* cells. Though this study shows the CPP itself can cross the membrane barriers of *C. albicans* with a small fluorescent label, more work is needed to evaluate the uptake of CPP-biomolecule fusion proteins in *C. albicans*.

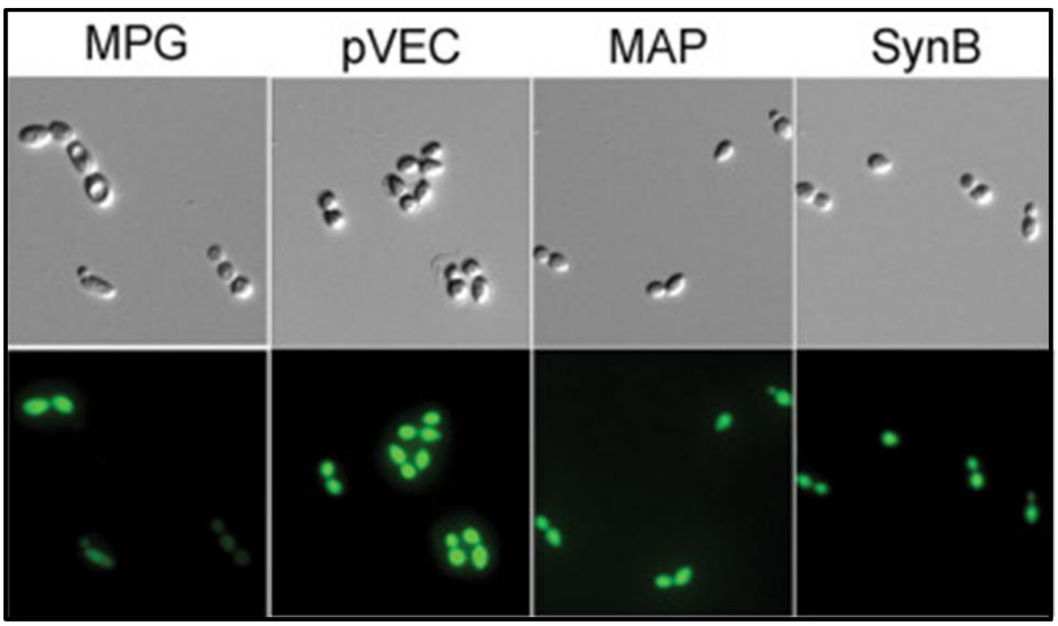

Figure 1.6. The translocation of certain CPPs into *C. albicans*. All the CPPs were fused to fluorescein dye to detect their cellular uptake via fluorescence microscopy. The green fluorescent indicated a successful translocation into *C. albicans*. Figure reprinted

with permission from Gong et al [11]. Copyright © 1999-2024 John Wiley & Sons limited.

Some of the CPPs have shown antifungal activity against certain fungi while remaining nontoxic against mammalian cells. Holm et al. tested the antifungal activity of CPPs against *Malassezia sympodialis*, a yeast that may contribute to skin disorders such as dandruff and atopic eczema [10]. In this study, the overnight culture of *M. sympodialis* was diluted to a designated concentration, mixed with CPPs in a 96-well plate, and then incubated for three days. The results showed that several CPPs, including Arg9, pVec, Tat, and penetratin, inhibit the cell growth of *M. sympodialis* at submicromolar concentrations without a significant impact on mammalian cells.

1.4 Strategies applied to improve protein expression

Despite several studies on CPPs, most of them focused on the CPP itself or the CPP-conjugated small molecules. The research on the translocation of CPP complexation with proteins is relatively limited. This study thus focused on the characteristics of CPP fusion to protein cargo.

As for the protein production, recombinant protein technology is one of the most convenient methods to acquire a great amount of protein. By transforming the gene of interest into the host cell, mainly *E. coli*, for its fast cell growth rate and well-constructed genetic background, the host will express lots of recombinant protein under certain induction conditions at a low cost. The other advantage of this technology is its flexibility. Recombinant protein technology easily cooperates with well-developed

DNA editing technology to alter recombinant protein constructs, such as adding and removing features. Therefore, all CPP-cargo constructs in this work were produced by recombinant protein technology.

1.4.1 Optimization of the induction conditions

Though there are several applications of CPP fusion proteins, it can be challenging to produce the fusions. Since there is no universal induction condition for all recombinant proteins, the induction parameters should be tuned and optimized based on the need and the characteristics of the protein of interest. Typically, the expression level is higher under higher induction temperature and lower induction time. During the optimization process, instead of changing one variable at a time, applying factorial design to the expression experiment can better describe the effect of multiple variables involved in the expression process [23].

Unfortunately, the expression level of CPP recombinant proteins can be low sometimes [11,23]. The cause of low expression may result from the characteristics of the CPP-fused protein, low solubility, and relatively high toxicity toward host cells. To reach higher expression level, Adhikari et al. applied a factorial experimental design to figure out the most beneficial induction condition of three CPP-recombinant protein design and had successfully optimized the production of all these proteins [23]. Their results verified the feasibility of tuning the expression of CPP-fused proteins by adjusting the induction conditions.

1.4.2 Addition of the glycine-serine linker (G_4S linker)

Besides optimizing the induction parameters, based on Gong et al., adding a linker between CPP and the carrying cargo proteins can also enhance the expression of certain CPP recombinant proteins [24]. In their study, a G_4S linker was included between the CPPs and the carrying cargo. Their result showed that the addition of the linker increased the yield of the purified CPP recombinant protein without reducing the translocation of the CPP recombinant protein into the targeted fungal cells. Furthermore, the linker itself did not alter the cytotoxicity of the protein construct, which makes it ideal to include the linker in CPP recombinant protein design in order to further explore the potential of CPPs.

1.5 Overview of the thesis

In this thesis, we constructed two different designs based on MAP, a CPP that shows potential in penetrating fungal cell membranes. We also optimized the induction condition to improve the expression of the recombinant protein. We attempted to purify the protein with a chromatography column. The detailed experimental process and strategy are described in Chapter 2, while the expression and purification results are discussed in Chapter 3. In Chapter 4, we resent the conclusions of our work and propose potential future work for further study of the possibility of the CPP-fusion protein.

Chapter 2: Materials and Methods

2.1 Overview of plasmid construction

Table 2.1. List of CPPs used in this study.

Name	Amino acid sequence	Molecular weight (Da)	Protein origin
MAP	KLALKLALKALKAALKLA	1876.0	Synthetic
MPG	GALFLGFLGAAGSTMGAWSQPKKKRKV	2807.4	Chimeric
pVec	LLIILRRRIRKQAHAHSK	2209.7	Natural-derived
SynB	RGGRLSYSRRRFSTSTGR	2100.3	Natural-derived

Table 2.2. List of plasmids. All the constructs were cloned into pET21(a)+ vector.

Plasmid name	Description
GFP-6xHis	Construct without CPP in the sequence. 6x-His tag was fused to the C terminus for analysis.
T7-GFP-G_4S-MPG	GFP fused to the N-terminus of MPG. This plasmid was used as the source of the plasmid backbone to prepare the constructs for this work.

T7-GST-FXa-MAP-G_4S-meGFP-6x His	The main construct for the CPP-cargo design of this study. This construct included a set of expression partners, GST and T7. GST and 6x His tag can be used for analysis and purification. This construct was first commercially synthesized by Genewiz/Azenta and used as the template for other CPP-first constructs.
T7-GST-FXa-MPG-G_4S-meGFP-6x His	The MPG version for the CPP-first design of this study. This construct was prepared via three overhang PCR reactions and oligonucleotide dimer insertion.
T7-GST-FXa-pVec-G_4S-meGFP-6x His	The pVec version for the CPP-cargo design of this study. This construct was prepared via two overhang PCR reactions and oligonucleotide dimer insertion.
T7-GST-FXa-SynB-G_4S-meGFP-6x His	The SynB version for the CPP-cargo design of this study. This construct was prepared via two overhang PCR reactions and oligonucleotide dimer insertion.
T7-FXa-6x His-meGFP-G_4S-MAP	The main construct for the cargo-CPP design of this study. This construct included a set of expression partners, GST and T7. GST and 6x His tag can be used for analysis and purification. This construct was first commercially synthesized by Genewiz/Azenta and used as the template for other cargo-first constructs.

T7-FXa-6x His-meGFP-G_4S-MPG	The MPG version for the cargo-CPP design of this study. This construct was prepared via three overhang PCR reactions and oligonucleotide dimer insertion.
T7-FXa-6x His-meGFP-G_4S-pVec	The pVec version for the cargo-CPP design of this study. This construct was prepared via two overhang PCR reactions and oligonucleotide dimer insertion.

Table 2.1 shows all the CPPs used in this thesis, while Table 2.2 provides a list of the plasmids used in this work. The T7-GST-FXa-MAP-G_4S-meGFP-6x His and T7-FXa-6x His-meGFP-G_4S-MAP plasmids were commercially synthesized and put into the pET21(a)+ plasmid by Genewiz/Azenta (Waltham, MA) and served as the template for CPP-cargo and cargo-CPP recombinant protein plasmid designs. Then, the sequence encoding MAP was substituted with the sequence encoding other CPPs (Table 2.1) to build up other CPP recombinant constructs via overhang polymerase chain reaction (PCR) amplification and oligonucleotide dimer insertion as described below.

2.2 Preparation of CPPs oligonucleotide insertion via overhang PCR amplification

This thesis applied overhang PCR amplification to prepare recombinant constructs for other CPPs, namely MPG, pVec, and SynB (Figure 2.1). The MAP recombinant constructs served as the first template for amplification in the PCR process. A set of forward and reverse oligonucleotides was designed to perform an overhang PCR reaction with several bases overlapping with the double-stranded template for orientation. During the PCR process, the polymerase recruits complement nucleotides to the overhang single-stranded oligonucleotides until the whole single-stranded DNA is properly complemented. The entire PCR process repeats several times to ensure sufficient amplification of the overhang PCR product. The PCR product can serve as the template for another overhang PCR reaction or be used as the DNA oligonucleotide insert for the subsequent experiment after the PCR clean-up process using the Wizard™ SV Gel and PCR Cleanup System kit (Promega, Madison, WI). To prevent the formation of secondary DNA structure and mispairing during the PCR process, the length of each oligonucleotide was limited to 50-60 bases.

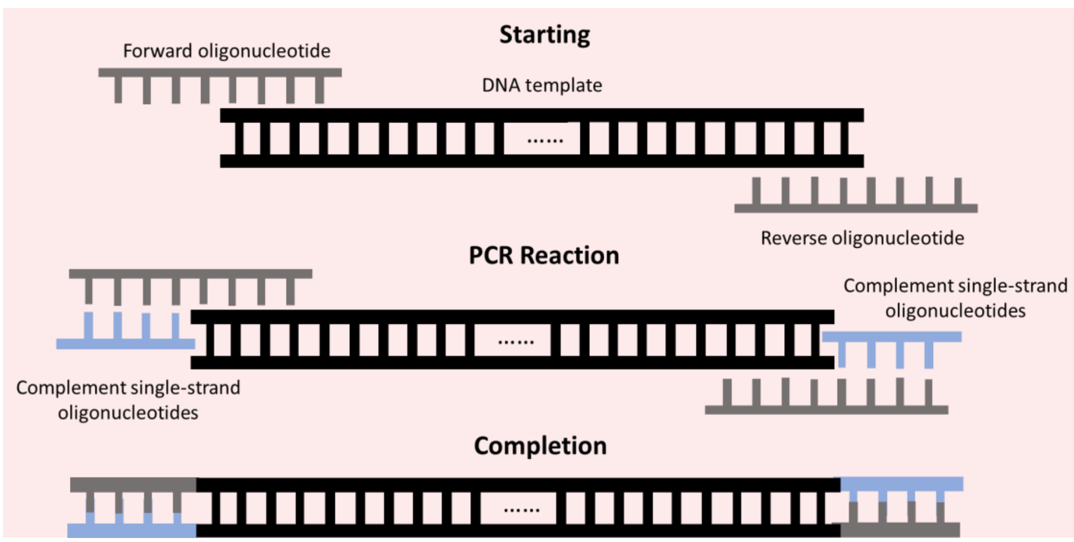

Figure 2.1. The schematic of the overhang PCR reaction. The overlapping bases with the fragmented template on the forward and reverse oligonucleotides serve as the orientation of the PCR reaction. Then the DNA polymerase recruits free nucleotides to form a complementary single-strand DNA to both the forward and reverse nucleotides to the end of both nucleotides. After the polymerization, the halfway PCR products overlap with other products with the same oligonucleotides and then are annealed into one final PCR product.

Table 2.3. List of oligonucleotides used for the preparation of CPP nucleotide insertion

Name	DNA sequence (from 5' to 3' end)
Oligonucleotides used for the CPP-cargo constructs	
Not1-GFP reverse	AGTGCGGCCGCTTTATATAATTC
MPG3-G_4S forward	TGCTTGGAGTCAACCAAAGAAGAAAGGTAAAGTAGAGC TCGGAGGCGG
MPG2-MPG3 forward	GGTTCCTCGGAGCAGCGGGGAGTACGATGGGTGCTTGG AGTCAACC
EcoR1-MPG1-MPG2 forward	AAAAGAATTCATCGAAGGTCGTGGAGCACTTTTCTTAGGG TTCCTCGGAGC
pVec2-G_4S forward	GTCGTATTCGTAAACAGGCACACGCACATAGCAAAGAGC TCGGAGGCGG
EcoR1-pVec1 forward	AAAAGAATTCATCGAAGGTCGTCTGCTGATTATTCTGAGGC GTCGTATTCGTAAAC
SynB2-G4S forward	GTCGTTTTTCCACAAGCACAGGACGTGAGCTCGGAGGC GG
EcoR1-SynB2 forward	AAAAGAATTCATCGAAGGTCGTCGTGGTGGTCGCCTGTCC TACTCCCGCCGTCGTTTTTC
BamH1-start-meGFP	GTCACGGATCCATGGTTAGTAAAGGTGAA
Oligonucleotides used for the cargo-CPP constructs	
HindIII-meGFP forward	AAGCTTGTTAGTAAAGGTGAAGAATTA

SacI-MPG1 reverse	CTCGAGTGAGCTCTTCATACTTTACCTTTCTTCTTTGGTT GACT
MPG1-MPG2 reverse	TTTGGTTGACTCCAAGCACCCATCGTACTCCCCGCTGCT CCGAGGAACCCTAAGAAAAGT
MPG2-MPG3-G_4S reverse	CTAAGAAAAGTGCTCCGAATTCGCTTCCACCGCCTCCTG CGGCCGCTTTA
SacI-pVec reverse	CTCGAGTGAGCTCTTCATTTGCTATGTGCGTGTGCCTGTT TGCGAATGCGGCGTCGCA
pVec-G_4S reverse	CGTCGCAGAATAATCAGCAGGAATTCGCTTCCACCGCCTC CTGCGGCCGCTTTA

Three overhang PCR reactions were needed to prepare the oligonucleotide insert for the MPG-cargo construct. For the first reaction, Not1-GFP reverse and MPG3-G_4S forward (Table 2.3) were used as the set of reverse and forward oligonucleotides, while the commercially synthesized MAP-cargo constructs served as the template for the amplification. After the PCR clean-up process, the product from the first PCR reaction was used as the template for the second overhang PCR, with the forward primer replaced with the MPG2-MPG3 forward oligonucleotide. As for the third overhang PCR reaction, the product from the second PCR reaction was used as the template and the forward primer was replaced with EcoR1-MPG1-MPG2 forward. The product from the third PCR process was the MPG-cargo oligonucleotide insert.

The other CPP-cargo and cargo-CPP oligonucleotide inserts were also prepared using a process similar to the one used to prepare the MPG-cargo oligonucleotide insert. The difference in the preparation for other oligonucleotide inserts was the primer used (which was specific to the CPP being inserted) and the number of PCR reactions needed. Table 2.4 shows all the primers needed for building up each insert and the PCR reaction needed.

Table 2.4. List of primers and number of overhang PCR reactions needed to prepare each CPP insert.

Name of the oligonucleotide insert	Number of overhang PCR reactions needed	Forward/reverse oligonucleotide used in each PCR reaction in experimental order.
The oligonucleotide inserts for CPP-cargo constructs		
MPG-G_4S-meGFP	3	MPG3-G4S forward/Not1-GFP reverse
		MPG2-MPG3 forward/Not1-GFP reverse
		EcoR1-MPG1-MPG2 forward/Not1-GFP reverse
pVec-G_4S-meGFP	2	pVec2-G4S forward/Not1-GFP reverse
		EcoR1-pVec1 forward/Not1-GFP reverse
SynB-G_4S-meGFP	2	SynB2-G4S forward/Not1-GFP reverse
		EcoR1-SynB2 forward/Not1-GFP reverse
The oligonucleotide inserts for CPP-cargo constructs		
meGFP-G_4S-MPG	3	HindIII-meGFP Forward/SacI-MPG1 reverse

		HindIII-meGFP Forward/MPG1-MPG2 reverse
		HindIII-meGFP Forward/MPG2-MPG3-G4S reverse
meGFP-G_4S-pVec	2	HindIII-meGFP Forward/SacI-pVec reverse
		HindIII-meGFP Forward/pVec-G4S reverse

2.3 PCR product insertion into plasmid

To prepare a CPP-cargo or cargo-CPP construct, a designated DNA oligonucleotide insert and a plasmid backbone were necessary (Figure 2.2). As shown in the following figures, both the DNA oligonucleotide inserts and the plasmid backbone from T7-GFP-G_4S-MPG include two restriction enzyme cutting sites in their sequences, BamH1 and Not1 for CPP-cargo the construct and HindIII and Sac1 for cargo-CPP the construct. After adding the corresponding restriction enzyme to the plasmid, these sites were digested by incubating in a 37°C water bath for 1 hour. Then, the backbone reaction was be loaded on a DNA agarose gel for gel electrophoresis to remove the short DNA fragment cut out by the enzyme. To recover the plasmid backbone on the gel, the DNA band was cut out by a razor and purified with the Wizard™ SV Gel and PCR Cleanup System (Promega). Then, the plasmid backbone and the DNA oligonucleotide inserts described above were mixed with T4 DNA ligase and the T4 ligase buffer (New England Biolabs; Ipswich, MA) in a PCR tube and incubated overnight at 16°C to ensure the quality of the ligation process.

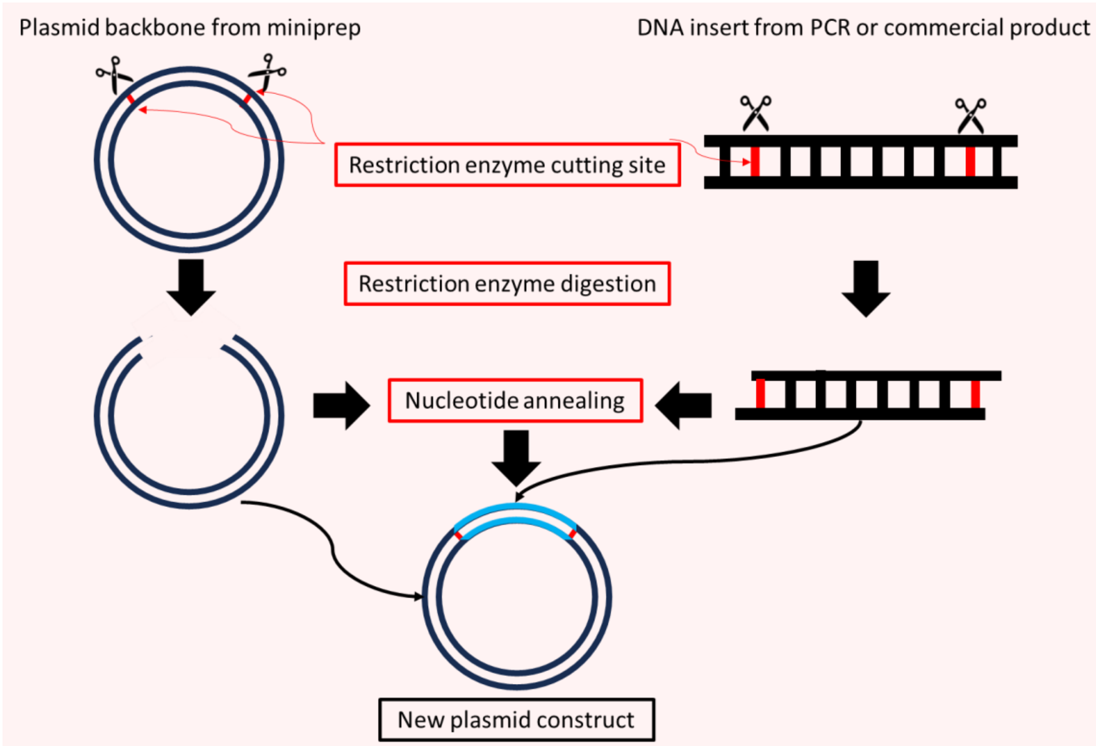

Figure 2.2. The schematic of plasmid constructs preparation by DNA oligonucleotide insertion. Both the plasmid backbone and the DNA insert from the overhang PCR reaction or commercial synthesis include restriction enzyme cutting sites for BamH1 at the 5’ terminus and Not1 at the 3’ terminus. After incubation with restriction enzyme at 37°C for 1 hour, it is possible to anneal the DNA oligonucleotide insert into the opening on the backbone recovered from gel electrophoresis and gel clean-up process. After the overnight ligation reaction, the new plasmid construct is built and is ready for transformation.

2.4 Transformation by electroporation

Each plasmid was transformed into four electrocompetent *E. coli* strains, including DH5α, BL21, BL21(DE3), and BL21(DE3)pLysS (Novagan; Lausanne, Switzerland), via electroporation. The DH5α strain was used for plasmid storage and plasmid sequencing for its high thermal stability and ability to achieve high transformation efficiency. All the other three strains are usually used for recombinant protein expression. The BL21 strain is a widely used non-T7 expression *E. coli* strain. Both BL21(DE3) and BL21(DE3)pLysS strains are used for protein expression involved with T7 polymerase. These two strains contain the λDE3 lysogen that carries the gene for T7 RNA polymerase under the control of the lacUV5 promoter, making the addition of isopropyl β-d-1-thiogalactopyranoside (IPTG) necessary to induce protein expression.

To transform the plasmid into target *E. coli* strains by electroporation, the plasmid acquired from the ligation step should was first be dialyzed against DI water for at least 20 minutes to reduce the salt concentration in the ligation mixture. Then, the desalted mixture would was be added to an electrocompetent cell suspension of the specific *E. coli* DH5α strain, which could be DH5α, BL21, BL21(DE3), or BL21(DE3)pLysS. After gentle mixing, the mixture containing ligated plasmid and the electrocompetent cells was loaded into a 1 mm electroporation cuvette (VWR; Radnor, PA). The mixture was shocked by the Gene Pulser Xcell instrument (Bio-Rad; Hercules, CA). The cell suspension was recovered for 1 hour with the addition of super optimal broth with catabolite (SOC) media (2% tryptone, 0.5% yeast extract, 10 mM NaCl, 2.5 mM KCl, 10 mM MgCl2, 10 mM MgSO4, and 20 mM glucose) at 37 $^{\circ}$C. The recovery process was done on a shaker with at 230 RPM before spreading on Luria Bertani (LB) agar plates (15 mg/mL agar, 10 mg/mL tryptone, 10 mg/mL NaCl, and 5 mg/mL yeast extract) containing 100 μg/mL of ampicillin.

To harvest the plasmid and prepare the cell's freezer stock, 2-3 colonies on the overnight LB agar plates were selected and added to LB liquid medium (10 mg/mL tryptone, 10 mg/mL NaCl, and 5 mg/mL yeast extract) containing ampicillin (100 μg/mL) and grown overnight. DNA was extracted from the overnight culture harvest using the Wizard Promoga miniprep kit. To confirm the DNA sequences, the plasmids were sent to Genewiz/Azenta for Sanger sequencing. A freezer stock was prepared from each overnight culture for long-term storage by mixing a 1:1 volume ratio of 50% glycerol and the overnight culture.

To express the recombinant protein in other strains, the DH5α cells containing the corresponding plasmid were cultured overnight. The plasmid was extracted from an overnight cell culture using the Wizard Promoga miniprep kit. Then the same electroporation steps were repeated to transformed the plasmid into BL21, BL21(DE3), and BL21(DE3)pLysS strains.

2.5 Protein expression

To express the recombinant protein, the cells containing the expression plasmid were first grown in LB medium overnight at 37 ⁰C with vigorous shaking at 230 RPM. The optical density at 600nm was measured for the overnight culture to normalize the subculturing conditions. Then, the cells were subcultured in a given amount of LB medium with 100 μg/mL of ampicillin (5 ml for expression test, 1000mL for further purification) with the optical density at 600nm set at 0.05. After growing the subculture for around two and half hours at 37 °C with vigorous shaking at 225 RPM, IPTG (Fisher Bioreagents) was added to a final concentration of 0.1 mM to induce the expression of recombinant proteins. To study the optimized conditions for protein expression, the induction times were 6, 10, and 24 hours at three temperatures, 37, 30, and 20º. After the induction time ended, the cells were harvested through centrifugation at 3700×g at 4 ℃ for 20 min. The supernatant was discarded, and the cell pellets were saved for further analysis.

2.6 Western blot

Western blotting was performed to test the expression level of different constructs under various expression conditions. The cell pellets harvested from a 5mL LB subculture were lysed by adding BugBuster Master Mix (EMD Millipore; Burlington, MA) to extract the soluble portion of the cells. The protein in the inclusion cell bodies was also recovered and kept as samples based on the BugBuster manufacturer's protocol. The sample normalization could be done by either protein concentration or total protein mass. The protein concentration in the sample was measured using a Nanodrop instrument (Thermo Scientific) to detect the absorbance at 280 nm. The normalized sample was mixed with sodium dodecyl sulfate polyacrylamide gel electrophoresis (SDS-PAGE) dye (0.05 M Tris-HCl, 0.1 M dithiothreitol (DTT), 8% (w/v) SDS, 1.5 mM bromophenol blue, and 1.075 M Glycerol) and loaded onto a gel for separation by sodium dodecyl sulfate (SDS). After SDS-PAGE separation, the proteins were transferred onto a polyvinyl difluoride (PVDF) membrane using a Trans-Blot Turbo instrument (Bio-Rad). After transferring, the membrane was soaked in 5% (w/v) non-fat dry milk in Tris-buffered saline containing Tween-20 (TBST; 0.1% Tween-20, 50 mM Tris-HCl pH 7.5, 150 mM NaCl) for an hour at room temperature or overnight at 4 ℃ to ensure sufficient blocking. Then, the membrane was washed three times with TBST to remove excess milk. The membrane was incubated with appropriate dilutions of the horseradish peroxidase (HRP)-conjugated anti-6×His tag antibody (Abcam; Boston, MA), HRP-conjugated anti-GFP antibody (Abcam), or HRP-conjugated anti-GST antibody (Abcam) at manufacturer-recommended concentrations for an hour at room temperature. After incubation, the membrane was washed 4-6 times with TBST buffer to remove non-specific binding or excess antibodies. Clarity Western ECL substrate (Bio-Rad) was added onto the membrane and incubated for 5 minutes. The visualization of protein bands on the membrane was done by chemiluminescence imaging on a ChemiDoc MP documentation system (Bio-Rad).

2.7 Protein extraction

To obtain cell lysate for purification of protein, cell pellets were harvested from two 1 L subcultures and resuspended with equilibration buffer (500mM NaCl, 50mM sodium phosphate (NaPB), pH 7.5) to a total volume of 25 mL. After resuspension, 25 μL of 100× protease inhibitor stock (MilliporeSigma; Burlington, MA) and 10 μL of benzonase nuclease (MilliporeSigma) were added to the suspension to prevent protein degradation and reduce viscosity, respectively. The cell suspension was physically lysed by a homogenizer cell disruption system (Avestin, Inc., Ottawa, Canada). The lysed suspension was centrifuged at 11400 × g for 20 minutes to remove insoluble cell debris from the supernatant containing our protein of interest. The supernatant was further centrifuged at 16000 × g for 20 minutes to minimize the insoluble fraction in the supernatant. After the second centrifugation, the clear supernatant, also called the lysate, was filtered through a 0.45 μm and 0.22 μm sterile filter and saved for further purification.

2.8 Protein purification

To obtain cell lysate for purification of protein, cell pellets were harvested from two 1L subcultures and resuspended with equilibration buffer (500mM NaCl, 50mM NaPB, pH 7.5) to a total volume of 25 mL. After resuspension, 25 μL of 100× protease inhibitor stock (MilliporeSigma; Burlington, MA) and 10 μL of benzonase nuclease (MilliporeSigma) were added to the suspension to prevent protein degradation and reduce viscosity, respectively. The cell suspension was physically lysed by a homogenizer cell disruption system (Avestin, Inc., Ottawa, Canada). The lysed suspension was centrifuged at 11400 × g for 20 minutes to remove insoluble cell debris from the supernatant containing our protein of interest. The supernatant was further centrifuged at 16000 × g for 20 minutes to minimize the insoluble fraction in the supernatant. After the second centrifugation, the clear supernatant, also called the lysate, was filtered through a 0.45 μm and 0.22 μm sterile filter and saved for further purification.

To prepare a GST affinity chromatography column, glutathione resin (GenScript; Piscataway, NJ) and appropriate columns (Bio-Rad) were used. Around 5mL of resin was loaded into each GST column. The column was equilibrated with 5 column volumes of the GST Equilibration/Wash Buffer (125 mM Tris-HCl, 150 mM sodium chloride; pH 8.0). After loading the lysate onto the column, the whole column was incubated for 1 hour on a rotator to ensure sufficient binding between protein and resin. After the incubation was completed, the flowthrough from the column was collected, and the column was washed with 5 column volume of the GST Equilibrium/Wash buffer, which was also collected as Wash 1. The washing step was repeated two more times to remove unbound protein, and the flowthroughs from each repetitive wash were Wash 2 and Wash 3. After the washing steps, the protein bound to the column was eluted using GST Elution buffer (125 mM Tris-HCl, 150 mM sodium chloride, 10 mM reduced glutathione from Thermo Scientific (Waltham, MA); pH 8.0), and the eluent was also collected as Elute 1. The elution step was also repeated, and the eluents from each repetitive elution were Elute 2 and Elute 3.

2.9 SDS-PAGE for purification analysis

SDS-PAGE was used to analyze the purification of the recombinant proteins. The samples were normalized by the protein concentration of the sample. After normalization, a 20 μL solution containing 1× SDS-dye was added to the samples, and the samples were heated at 98 °C for 5 min to denature the protein. For each sample, 2 μL of denatured protein solution was loaded to one of the ten lanes on an Any KD Mini-Protein TGX 10-well gel (Bio-Rad) along with a molecular weight ladder (Precision Plus Protein™ Dual Color Standards; Bio-Rad). The gel was run at 200 V for 30 mins to separate proteins based on their size. The gel was stained using Bio-Safe Coomassie (Bio-Rad) and imaged by a ChemiDoc MP documentation system (Bio-Rad).

Chapter 3: Results and Discussion

3.1 Plasmid construct

Two different construct designs were built for this thesis to test the expression of the CPP-cargo protein complex and to study the effect of the location on the CPP on recombinant protein expression (Figure 3.1). The main difference between these two designs is the sequential order of the CPP and the cargo. The CPP is at the N-terminus of the cargo for the CPP-cargo design, while the CPP is at the C-terminus of the cargo for the cargo-CPP design.

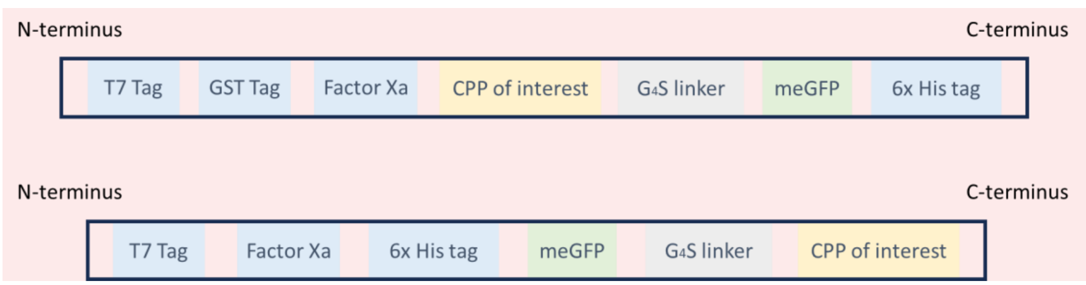

Figure 3.1. This work used two CPP recombinant protein designs: (a) CPP-cargo design, with the CPP at the N-terminus of the cargo, and (b) cargo-CPP design, with the CPP at the C-terminus. The T7 tag was included in both designs to improve the expression. Glutathione S-transferase (GST) and 6x His tags were used for purification.

3.2 CPP and cargo selection

3.1.1 Green fluorescent protein

The monomeric enhanced green fluorescent protein (meGFP) was selected as the cargo in the recombinant protein construct in this work with consideration of the ease of expression, the ability for quantification analysis, and the stability. Green fluorescent protein (GFP) is widely used in biomedical and biotechnology applications, such as protein fusion and subcellular localizations, as a marker for straightforward quantification and characterization by fluorescent microscopy or flow cytometry. GFP was first discovered and isolated from *Aequorea victoria*, a jellyfish species with bioluminescence present in North America [28]. The core motif of the GFP is a p-hydroxy benzylidene 2,3-dimethyl imidazolinone chromophore, which is densely packed with hydrogen bonds inside a barrel-shaped structure that creates a distinct absorbance and emission of light. For wild-type GFP, the chromophore absorbs visible light with a wavelength of 475 nm and emits fluorescence at 395 and 503nm [28,29]. meGFP is a variation of GFP. The fluorescence strength is improved by introducing two point mutations in the chromophore, which substitute the 56th amino acid serine with threonine and the 54th amino acid phenylalanine with leucine [30]. The modifications lead to a single excitation peak at 489 nm. The oligomerization tendency is also reduced in meGFP compared with wild-type GFP [31], making meGFP an ideal biomarker for long-term expression.

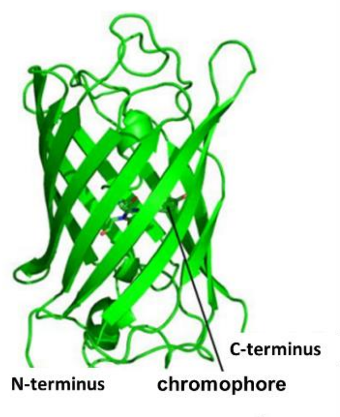

Figure 3.2. The crystal structure of GFP [29]. The chromophore is buried inside a β-barrel structure. The hydrogen bonding between the chromophore and the residues on the β-barrel stabilizes the structure and protects the chromophore from the bulk solvent. Figure reprinted with permission from Kong et al. [29]. Copyright 2020 Elsevier B.V.

3.2.1 Cell-penetrating peptides MAP, MPG, pVec, and SynB

This work focused on producing plasmids for the expression of CPP-cargo constructs and the optimization of the expression of CPP-cargo conjugated constructs. Four CPPs were selected as the CPPs of interest for their potential to serve as vehicles in the new drug delivery system for fungal cells: MAP, MPG, pVec, and SynB (Table 2.1). All these CPPs have shown the translocation into C. albicans in previous research [11, 23, 24].

MAP, first designed by Steiner et al. to study lipid interfacial interactions [32], is a model cell-penetrating peptide with an α-helical structure. Both hydrophobic and hydrophilic residues are on opposite sides of the helix, giving MAP the nature of secondary amphipathicity. The difference between primary and secondary amphipathicity lies in the its amphipathic mechanism [52]. Primary amphipathic peptides have both hydrophobic and hydrophilic residues in the primary structure, while secondary amphipathic peptides obtain amphipathicity via conformation change through its interaction with lipids [52]. The α-helical structure of MAP enables MAP to get close to a lipid membrane at temperatures between 25-55ºC [33,57]. The overall net positive charge of 5 allows MAP high stability in physiological conditions and a low blood clearance rate [33, 57]. MAP can utilize multiple translocation mechanisms, including direct penetration and endocytosis, depending on the design of MAP recombinant protein, the existence of fluorescent dye, and environmental conditions [33]. All these characteristics make MAP a promising delivery vehicle with penetration in a variety of cells; at least 50% of uptake in certain cell lines was detected even below 0ºC temperature [11, 34].

MPG is a primary amphipathic peptide consisting of three domains: an N-terminal hydrophobic motif, a C-terminal hydrophilic lysine-rich domain, and a linker domain connecting these domains [35]. The hydrophilic motif, derived from the nuclear localization sequence of simian virus 40 large T-antigen, is responsible for the solubility of the MPG recombinant protein and the intracellular trafficking. In contrast, the hydrophobic motif, derived from the fusion sequence of the HIV glycoprotein 41, is required for cell membrane targeting and cellular uptake. The linker motifs between these two motifs give some flexibility in the peptides, which is important for carrying macromolecules [35]. MPG has several successful applications as a carrier to deliver plasmid or oligonucleotides [36]. Yet, its potential for protein delivery remains to be explored.

Derived from vascular endothelium cadherin, a protein that plays a crucial role in transferring information from the extracellular environment, pVec consists of three domains: a hydrophobic N-terminus, a hydrophilic C-terminus, and an arginine-rich middle region [37,38]. The translocation of pVec can be via direct penetration facilitated by its hydrophobic N-terminus. The penetrating process is energy- and receptor-independent, enabling the translocation of pVec to various cell lines [37].

SynB, a cationic peptide derived from the antimicrobial peptide protegrin 1 [39, 40], can translocate into cells via the endocytic pathway. SynB has been used to deliver cargo with low molecular weight, such as dalargin and nanoparticles, through the mammalian brain-blood barrier [39]. Yet, the research on SynB as a delivery tool into other cell lines is still limited and needs further study.

3.3 Tag and functional proteins included in the protein constructs

Besides the CPPs and meGFP, several tags and functional proteins were included in the constructs. These additional elements in the construct could either improve the expression of recombinant proteins or facilitate the analysis and purification process after protein expression.

3.3.1 Bacteriophage T7 epitope tag (T7 tag)

The T7 tag, consisting of 11 amino acids (MASMTGGQQMG), can be included at the N-terminus of an expressed recombinant protein as an affinity tag and expression partner [41]. It can facilitate the high-titer production of the recombinant protein while preserving the function of the protein of interest and other tags included in the construct [42]. T7 tag was included in all constructs in this work as a part of the pET expression vector.

3.3.2 Glutathione S-transferase tag (GST tag)

GST tag, a 26 kDa protein, is another common affinity tag included in recombinant protein for purification by GST resin chromatography column. The GST fusion protein usually shows a high expression level in *E. coli*, even for highly toxic proteins. However, the drawback of the GST tag is its tendency to accumulate protein in inclusion bodies, which makes purification more challenging [41]. The GST tag was only included in the CPP-cargo construct to test if this tag could function as an expression partner for CPP recombinant protein.

3.3.3 Factor Xa site

Factor X is the zymogen of a serine protease, while the activated enzyme (factor Xa) is an Arg-specific serine protease. Factor Xa can be cleaved by factor Xa protease after the arginine residue in its preferred cleavage site Ile-Glu/Asp-Gly-Arg. The cleavage of factor Xa upstream of the protein preserves the activity and the structure of the downstream protein, making it a common tool in recombinant protein design [43, 44].

This functional protein was included in all structure in the N-terminus of our fusion protein of interest, which gave the CPP recombinant protein more flexibility as the expression partner and T7 tag can be removed from the final purified protein.

3.3.4 Hexahistidine tag (6x His tag)

The 6XHis tag enables the binding of tagged proteins to various metal ions, including Co^{2+}, Ni^{2+}, Zn^{2+}, and Cu^{2+}, which can be used for purification with the affinity column [45]. Since the 6xHis tag rarely interacts with other proteins or forms an accumulation, its inclusion is commonly seen in recombinant protein structures. This tag was included in all constructs used in this work.

3.3.5 G_4S linker

Previous research in our group showed that a G_4S linker between the CPP and the cargo could effectively improve the expression and purification of CPP recombinant protein with no significant negative effects on cellular uptake [24]. The G_4S linker was included in all constructs in this work to improve expression.

3.4 Construct cloning

Except for the MAP-cargo and cargo-MAP constructs that were commercially synthesized, attempts were made to prepare all the other constructs from overhang PCR reaction and oligonucleotide insertion. The MPG, pVec, and SynB constructs failed for both CPP-Cargo and Cargo-CPP orientations. Failures could be a result of the gene encoding CPP recombinant constructs may have formed secondary DNA structures, which could cause problems during plasmid construction Also, the high toxicity of the CPP constructs, which potentially inhibited the growth of the host cell during transformation. In fact, cloning CPP recombinant constructs is a consistent challenge for this work, and previous research within our group using multiple cloning methods has failed for unclear reasons. Considering the failure of the other constructs, the focus of this work was to optimize and compare the expression of the two MAP recombinant constructs.

Table 3.1. Characteristics of MAP constructs.

Construct Name	Number of base pairs for the corresponding gene (bp)	Protein molecular weight (kDa)
GST-MAP-G_4S-meGFP	1569	58.03
meGFP-G_4S-MAP	911	33.7

3.5 Recombinant protein expressions

All the CPP recombinant protein constructs were expressed through the pET system. pET system is one of the most powerful systems for recombinant protein expression in *E. coli*. Target genes cloned in pET plasmids were controlled by strong T7 transcription and translation signals, enabling recombinant protein expression by induction with T7 RNA polymerase in the host cells [47]. For both BL21(DE3) and BL21(DE3)pLySs strain, the T7 RNA polymerase was under strict control of the lacUV5 promoter, making the addition of IPTG necessary to induce the polymerase. This characteristic was beneficial since the toxicity of CPP recombinant protein may affect cell growth.

Since the absence of T7 RNA polymerase in the cell should prevent expression from pET plasmids in the BL21 strain, it served as a negative control of the expression experiment and analysis.

3.5.1 Comparison of expression of two MAP constructs

A Western blot was performed to directly compare the expression between the two MAP constructs to study the combinational effects of the cargo location and the tags included in the construct on the expression of MAP recombinant protein. Both MAP recombinant proteins were expressed in BL21(DE3), the strain that showed the highest expression for both constructs and the induction conditions were set to be 37°C and 6hr.

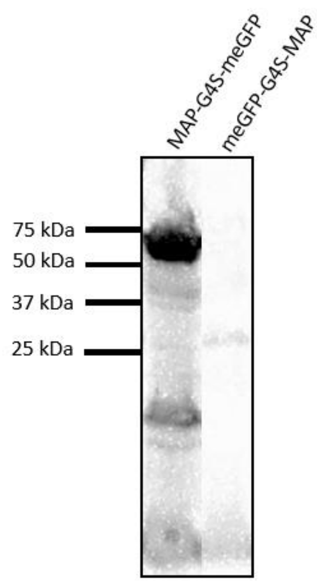

Figure 3.3. Comparison of expression of two MAP constructs in this work. Both constructs were expressed in BL21(DE3) strain at 37ºC for 6hr. After the induction, an equivalent volume of both sample lysates was harvested, run on a gel, and transferred on one membrane for Western blot. After being stained with α-GFP, the blots were

imaged and the respective exposure time was optimized by the ChemiDoc MP documentation system (Bio-Rad). The figure shows the representative lanes on the blots.

The expression of GST-MAP-G_4S-meGFP was significantly stronger than that of meGFP-G_4S-MAP (Figure 3.3). This result suggests that the inclusion of a GST tag in the MAP recombinant construct may have improved the protein expression to a great extent. However, since the GST tag was inclined to be cleavage by the proteases, the purification process of GST-included constructs could be more challenging. The sequential order of MAP and cargo may also have been a contributing factor to the difference in expression level. As the cargo protein, meGFP, was moved to the N-terminus of the construct before MAP, the expression of the recombinant construct was significantly decreased, which was aligned with results from previous research conducted within our group [23]. To reach a high-level expression of MAP recombinant construct, the inclusion of the GST tag and the sequence with MAP on the N-terminus of cargo protein is recommended.

3.5.2 Expression of GST-MAP-G_4S-meGFP

(a)

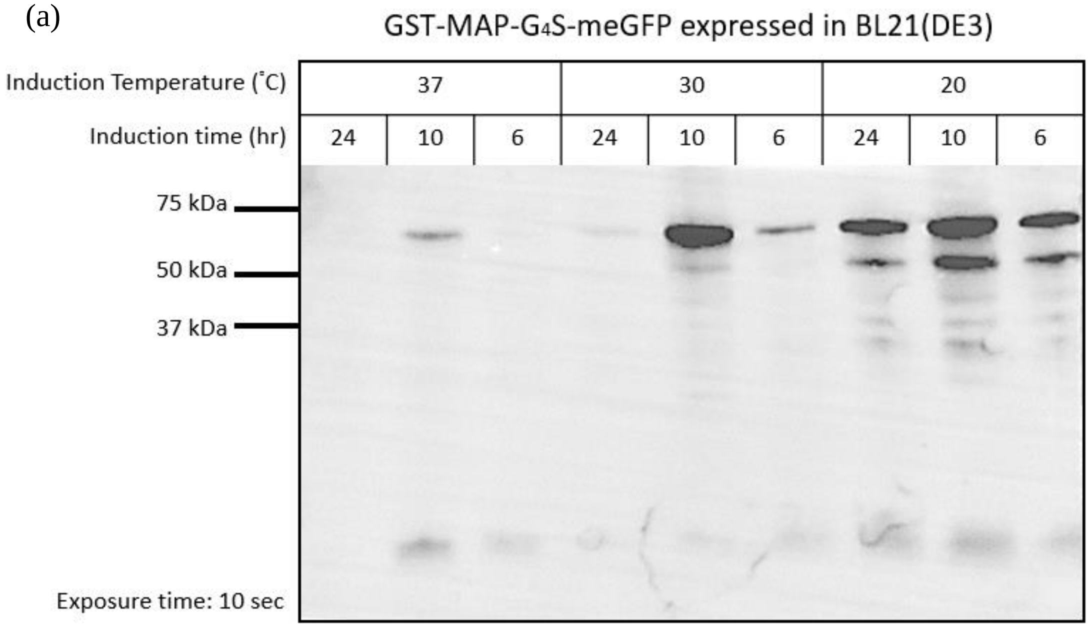
GST-MAP-G4S-meGFP expressed in BL21(DE3)
Induction Temperature (˚C)
37
30
20
Induction time (hr)
24
10
6
24
10
6
24
10
6
75 kDa
50 kDa
37 kDa
Exposure time: 10 sec

(b)

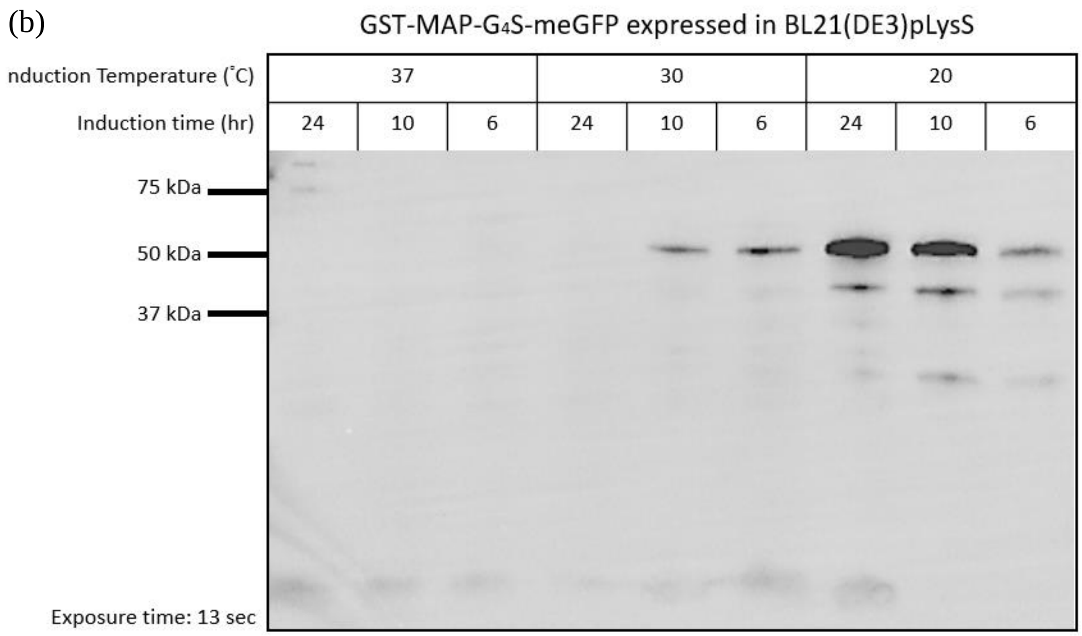
GST-MAP-G4S-meGFP expressed in BL21(DE3)pLysS
nduction Temperature (˚C)
37
30
20
Induction time (hr)
24
10
6
24
10
6
24
10
6
75 kDa
50 kDa
37 kDa
Exposure time: 13 sec

(c)

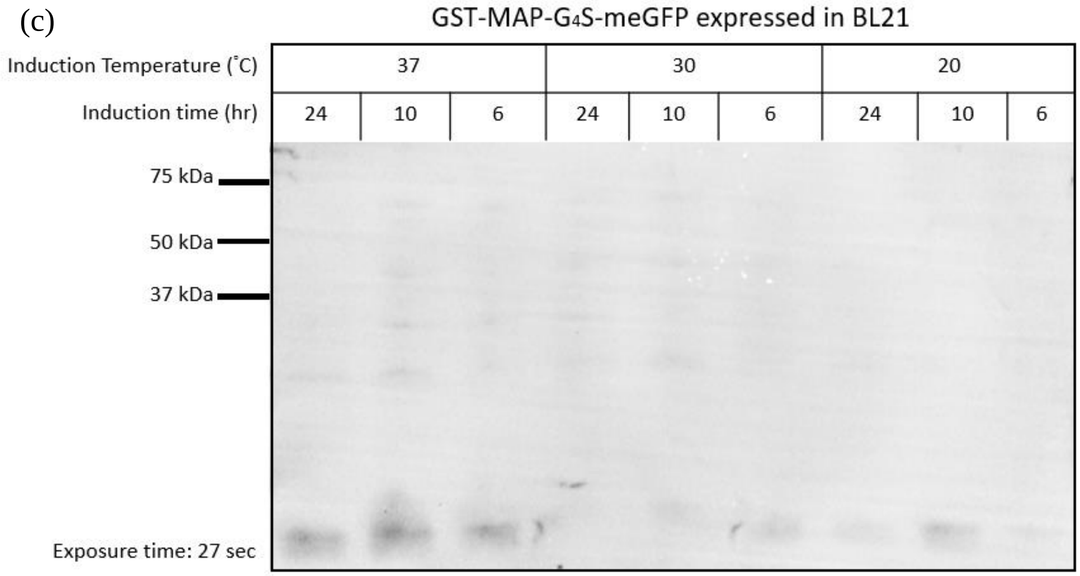

Figure 3.4. Western blot for expression of GST-MAP-G_4S-meGFP (58 kDa) in (a) BL21(DE3), (b) BL21(DE3)pLysS, and (c) BL21. Each of the three blots contains 9 samples with designated induction temperatures from 20-37°C and time from 6-24hr. After stained with α-6xHis, the blots were imaged and the respective exposure time is noted for each panel.

To tune the induction parameters for optimizing CPP protein expression, the expression of both MAP constructs was induced at 37, 30, and 20°C. For each induction temperature, the expression was induced for 6, 10, and 24 hours. GST-MAP-G_4S-meGFP could be effectively expressed in both BL21(DE3) and BL21(DE3)pLysS strains (Figure 3.4 a, b), while only a faint band was observed in the BL21 strain (Figure 3.4 c), which could be the non-specific staining bands present in all samples. These results indicated that the pET expression system worked well for this construct. A minor protein band with a size around 40 kDa was observed on both BL21(DE3) and BL21(DE3)pLysS blots in addition to the expected band, suggesting cleavage of the recombinant protein construct. Since the size of the GST tag was around 25 kDa, it was most likely that a portion of the GST tag in the recombinant protein was cleaved by the proteases present in the host cells.

3.5.3 Expression of meGFP-G_4S-MAP

(a)

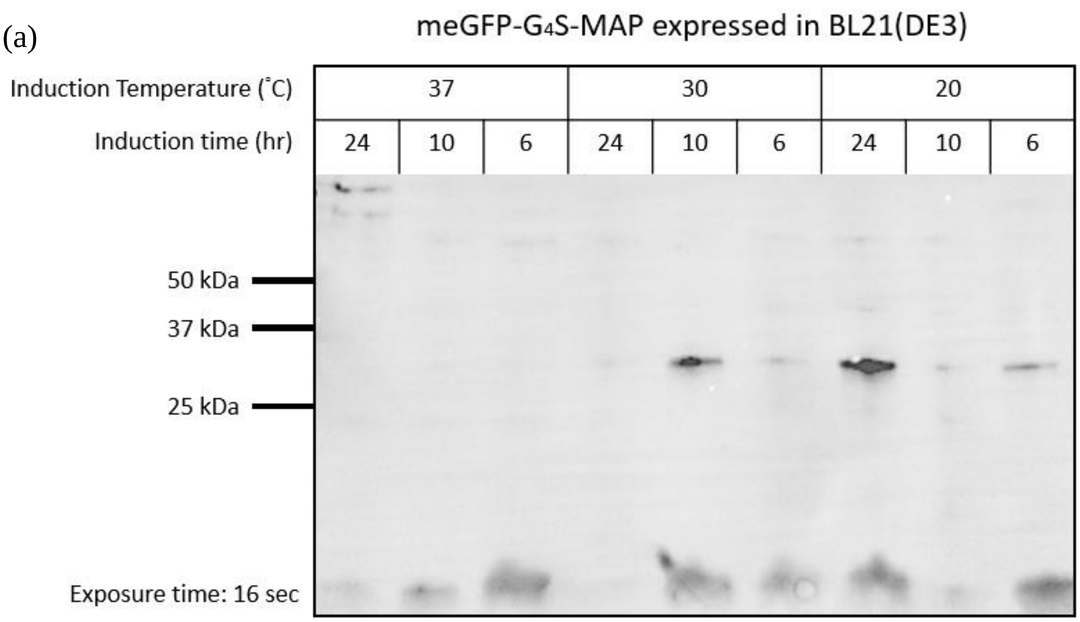

(b)

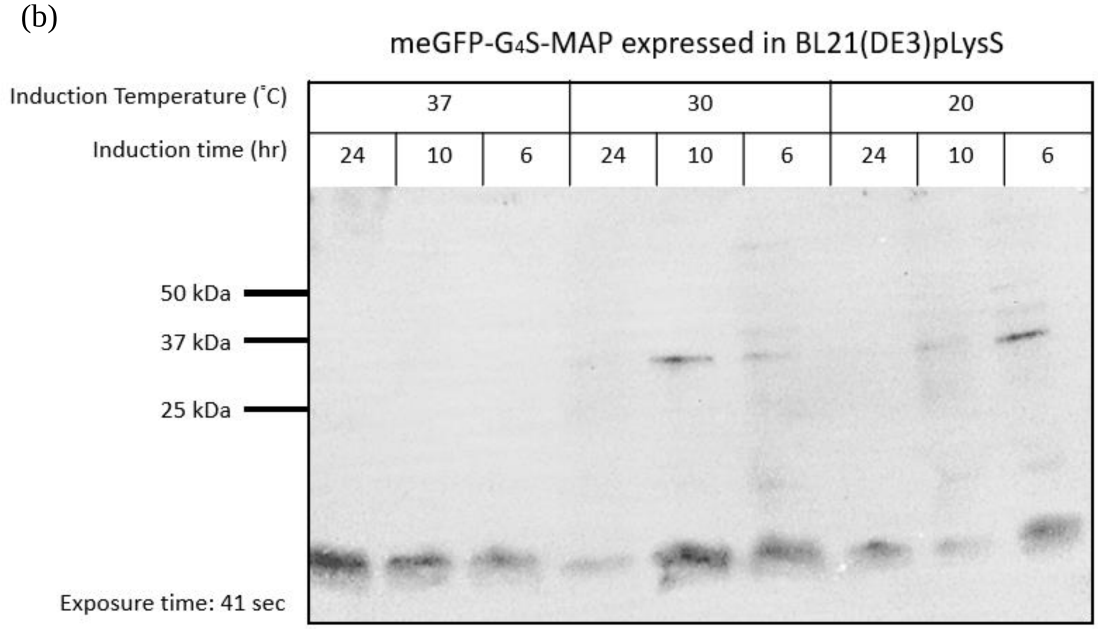

(c)

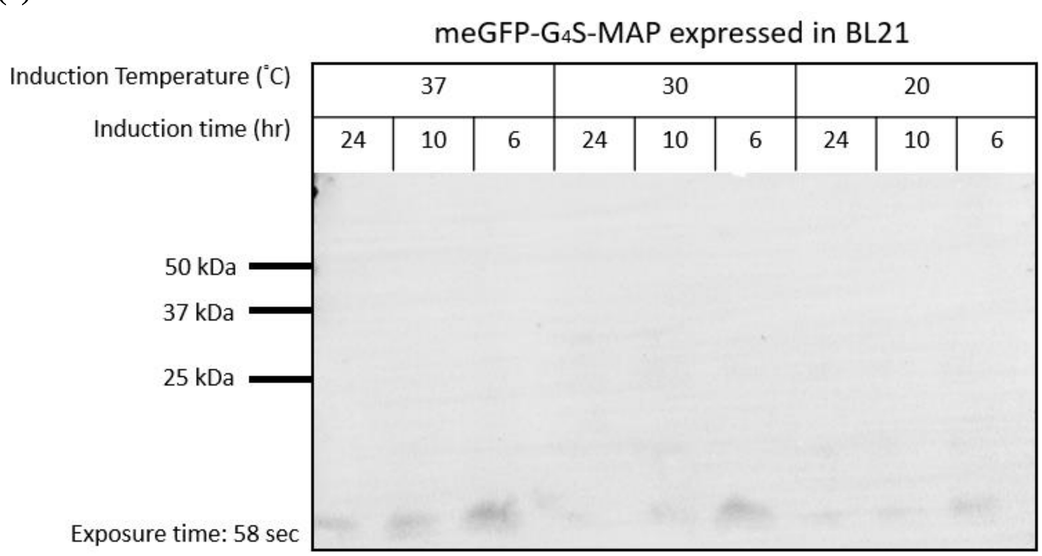

Figure 3.5. The Western blot for expression of meGFP -G_4S- MAP in (a) BL21(DE3), (b) BL21(DE3)pLysS, and (c) BL21. Each of the three blots contains 9 samples with designated induction temperatures from 20-37°C and time from 6-24hr. After stained with α-6xHis, the blots were imaged and the respective exposure time was optimized by the ChemiDoc MP documentation system (Bio-Rad).

The results of meGFP-G_4S-MAP expression were very similar to those obtained from GST-MAP-G_4S-meGFP expression. The expression of meGFP-G_4S-MAP can only observed in both BL21(DE3) and BL21(DE3)pLysS strains (Figure 3.5 a b), indicating that the pET expression system could effectively express this construct as well. However, the expression of this construct in BL21(DE3)pLysS was much lower than in BL21(DE3), which made longer exposure time necessary for band visualization. The expression level tended to be higher at lower induction temperatures with longer induction time. However, the trend was not as clear as the trend observed in the expression of GST-MAP-G_4S-meGFP. The highest expression level was obtained from the BL21(DE3) strain sample with 24 hours of induction at 20^{o}C.

<u>3.6 Recombinant protein purification</u>

The GST-MAP-G_4S-meGFP construct was selected for initial attempts at purification because of its high expression. After expression, the cells were harvested and then physically lysed, releasing soluble recombinant protein. To purify the protein from the lysate, a purification strategy with a combination of two chromatography columns was proposed. The cell lysate was first loaded to a GST affinity column, enabling the removal of the impurities without the GST tag. Then the factor Xa cutting site was cleavage by enzymes to remove the GST tag from the final product. After the cleavage, the protein was loaded onto an Immobilized metal affinity chromatography (IMAC) column to remove the impurities without a 6xHis tag (Figure 3.6). All the flowthroughs, washouts, and eluents from the column were collected and visualized on a gel.

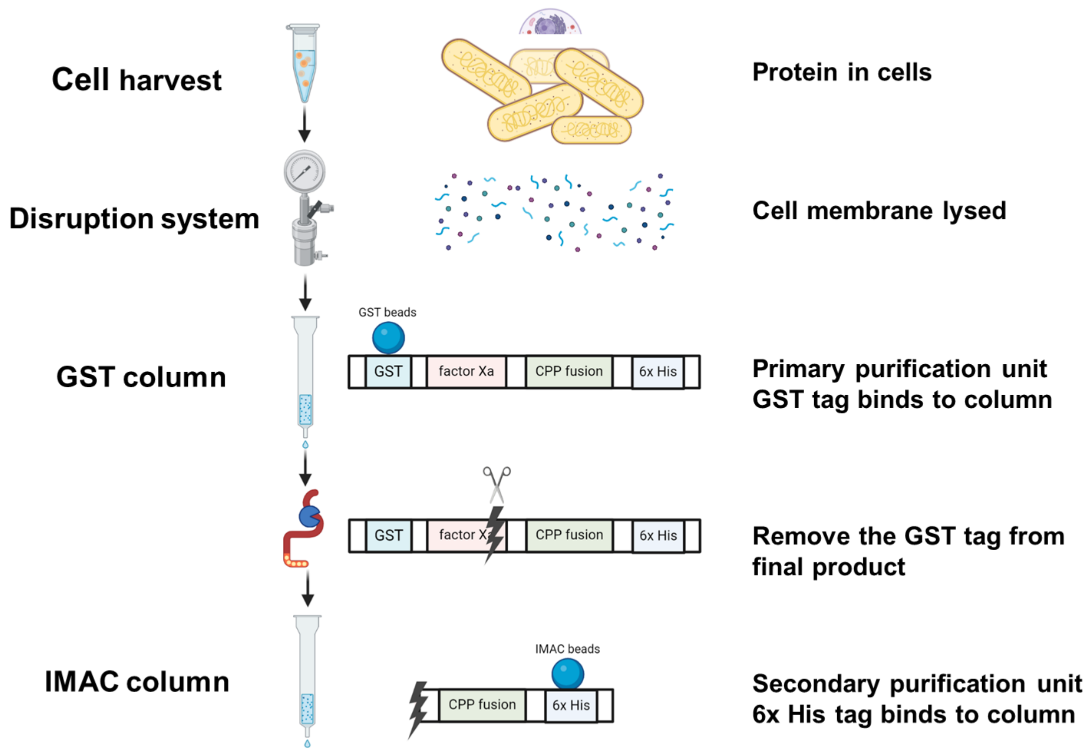

Figure 3.6. The Schematic of the purification strategy. The GST-MAP-G_4S-meGFP harvested from cell culture (a) first entered the cell disruption system to lyse the cell membrane (b). The cell lysate was loaded to a GST column to remove the impurities without a GST tag (c). The eluent from the GST column was treated with factor Xa protease to cut out the GST tag on the N-Terminus of the recombinant protein (d).the second purification was don't by IMAC column (e), the impurities without 6x His tag were removed. Figure created with BioRender.com.

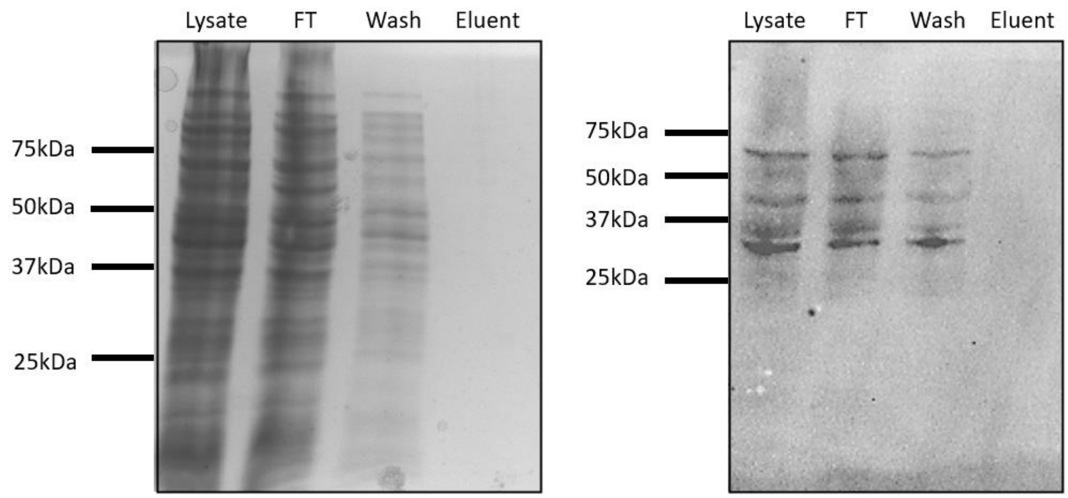

Figure 3.7. The Coomassie-stained gel (a) and Western blot stained with α-6xHis (b) for the GST column purification. The sample was collected from the column in each column purification step.

The results from the first purification unit, the GST column, showed that most of the protein was lost in the flowthrough and washout (Figure 3.7), indicating a weak interaction between GST resin and GST-MAP-G4S-meGFP protein. This could result from the 3D structure of the recombinant protein providing steric hindrance that prevented the GST tag in the construct from interacting with the GST resin beads. The low yield from the GST column prevented further purification based on our original purification strategy. An alternative column to the GST column will be necessary as a primary purification unit to purify this protein.

Chapter 4: Conclusions and Future Work

4.1 Conclusions

In this study, the combinational effects of several factors, including the inclusion of the GST tag, the order of MAP and cargo in the protein sequence, the host cell strains, and the induction time and temperature were evaluated to improve the expression of a fusion of the CPP MAP to meGFP. The GST tag significantly improved the expression of MAP recombinant protein, yet it also led to more impurities with a size smaller than the protein. The construct with GST and MAP at the N-terminus of the cargo showed a higher level of expression than that with MAP at the C-terminus of the cargo. The BL21(DE3) *E. coli* strain was identified as the most productive strain in the expression of MAP recombinant protein. As for the induction conditions, MAP recombinant protein could be expressed better at 20 ºC for an induction time of 24 or 10hr. This finding enables the generalization of an expression platform for MAP-meGFP recombinant proteins. As for the downstream processing of MAP recombinant protein, the GST column was not an effective purification unit due to weak binding between the protein and GST resin. On the other hand, there were several attempts to clone other CPP cargo constructs, including MPG, pVec, and SynB. All these clones failed in this work, indicating alternative production mechanisms or cloning methods could be necessary to produce the other CPP recombinant proteins. Our results can serve as a starting point for a generalized expression platform for other CPP-cargo fusion proteins.

4.2 Future work

4.2.1 A robust purification strategy for MAP recombinant protein

The GST column purification didn't cooperate reasonably for GST-MAP-G_4S-meGFP protein. Our result showed that most of the protein was lost during the loading and washing, indicating an alternative purification strategy is needed. Considering that the IMAC column still works for this construct (Figure 4.1), IMAC can be used as the primary purification step in the purification process. After cleaving the factor Xa by the protease, the protein can be purified with a size exclusion chromatography (SEC) column, which separates the proteins and impurities based on the size of the molecules, to remove the GST tag. Another option is substituting the GST tag with the maltose-binding protein (MBP) tag, a common affinity tag that helps recombinant protein expression. Previous research within our group also showed that the MBP tag could be effective in improving the CPP recombinant protein expression [23]. However, the cost of amylose resin, the critical material for an MBP chromatography column, is much higher than the GST resin, rendering this purification strategy less economical.

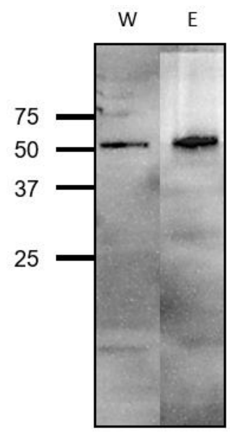

Figure 4.1. The representative purification results for GST-MAP-G_4S-meGFP by IMAC purification. The wash (W) and eluent (E) were collected from the column and run a gel for Western blot. The blot was stained with α-6x His and imaged with the respective exposure time optimized by the ChemiDoc MP documentation system (Bio-Rad).

4.2.2 Translocation of MAP-meGFP into *C. albicans*

The expression for MAP recombinant proteins was optimized in this research. The next step is to test the translocation of this construct after purification. For the translocation experiment, *C. albicans* cells can be incubated with MAP-G_4S-meGFP at a specific concentration for a given incubation period. After incubation, a cell viability assay can test the toxicity of the recombinant protein, while the translocation can be evaluated by flow cytometry and fluorescence microcopy.

4.2.3 Alternative protein expression system: cell-free protein synthesis (CFPS)

Considering the negative effects on CPP recombinant protein expression due to its toxicity, an alternative noncellular based expression could potentially reach higher production of CPP recombinant proteins. CFPS is a technique that allows a recombinant protein to be expressed outside of living cells. A CFPS system contains the polymerases, energy source, cell lysate, amino acids, and other cofactors required for protein expression, allowing higher flexibility and rigid control in expression experiments. With CFPS, there is no need for living cells for expression, which greatly undermines the effects of the toxicity of CPP recombinant proteins. However, this technique is relatively new and still in development. Optimization of all parameters in the CFPS system to reach high expression of CPP recombinant protein would be necessary, along with scaling up the production in CFPS system to get sufficient protein for translocation experiments.

Appendices

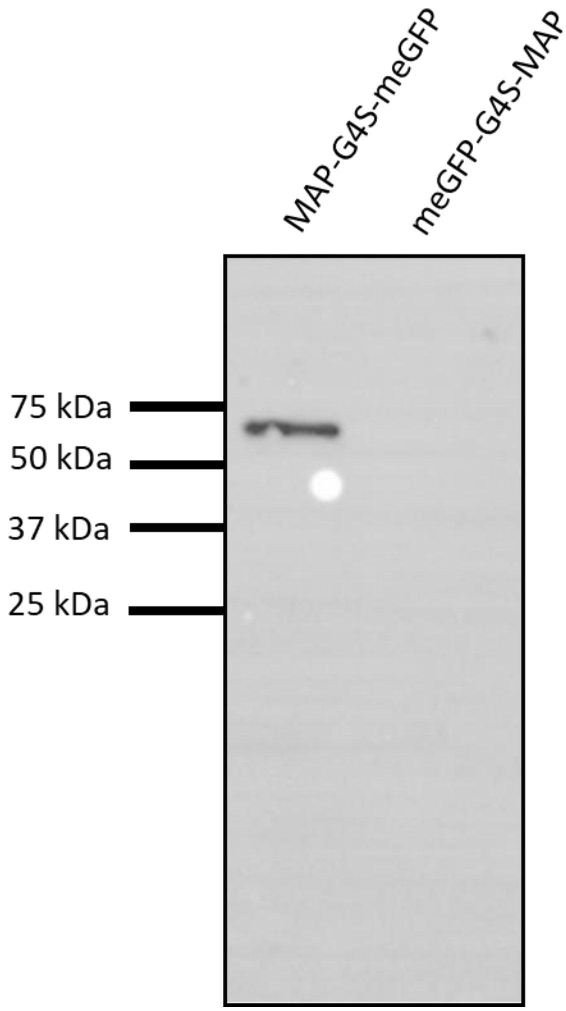

Figure A.1. Western blots for MAP recombinant protein expressed in CFPS kit.

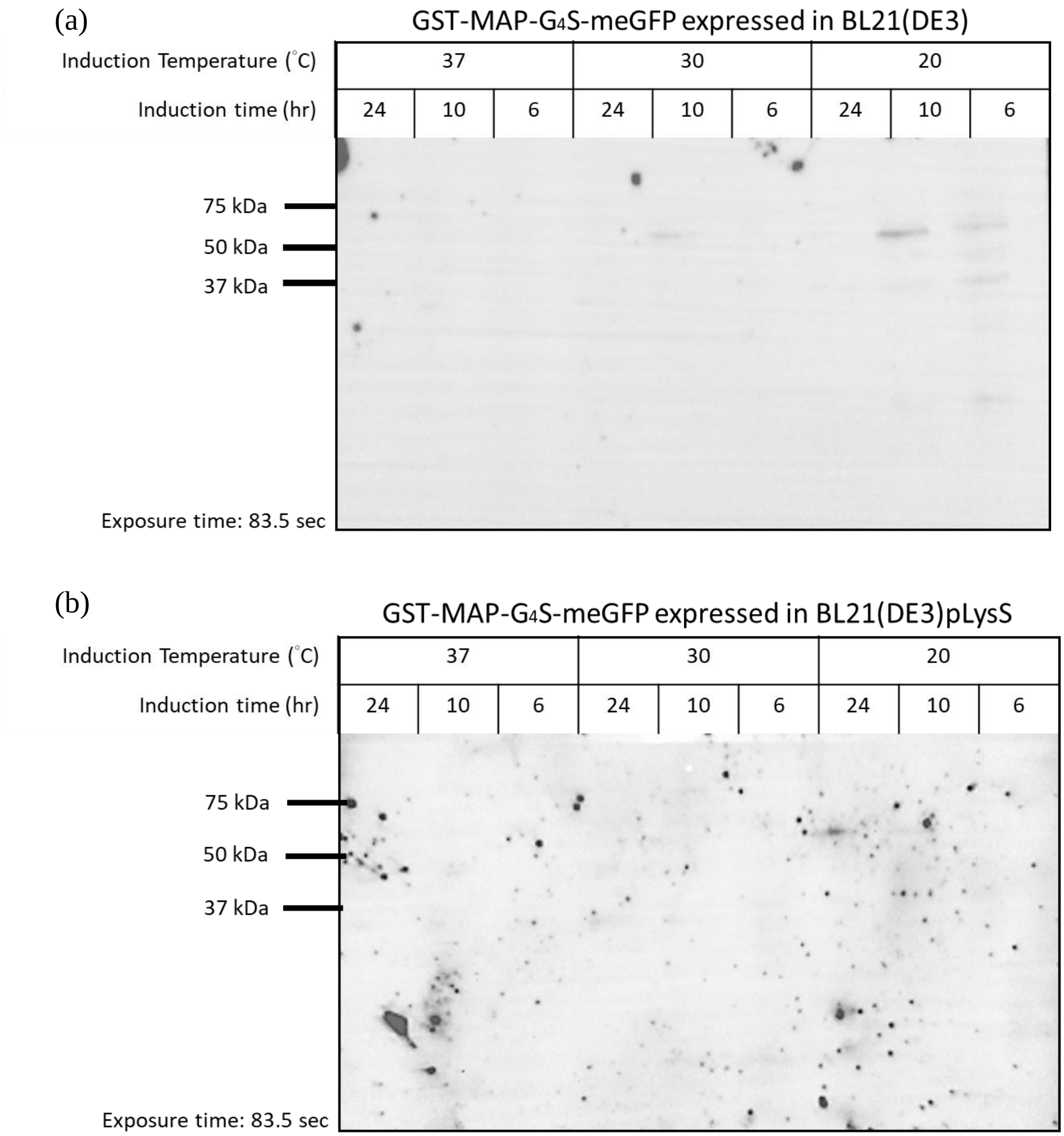

Figure A.2. Duplicate Western blot for expression of GST-MAP-G4S-meGFP (58 kDa) in (a) BL21(DE3), (b) BL21(DE3)pLysS.

(a)

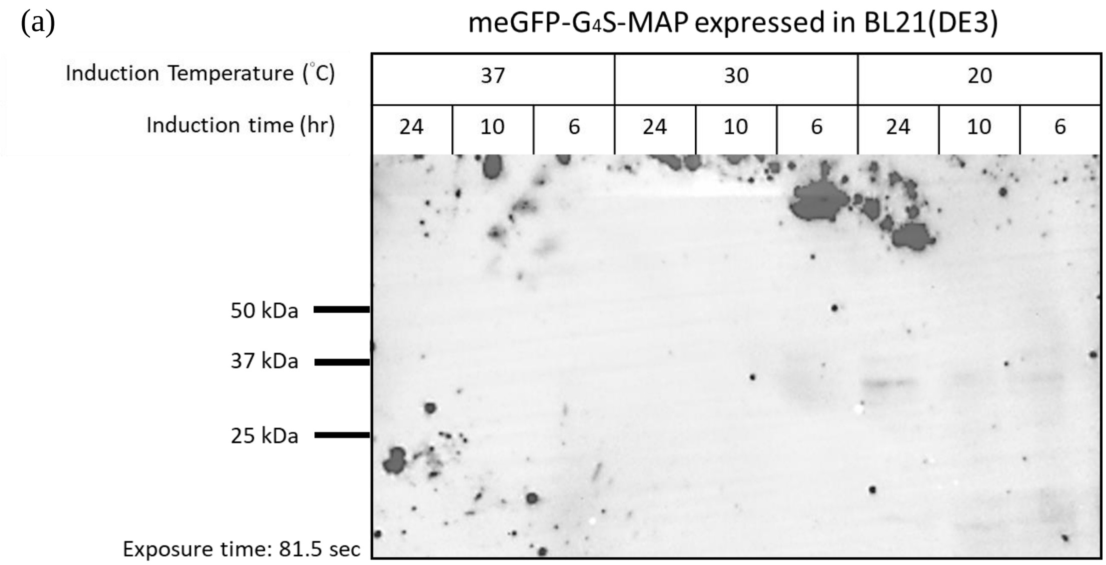

(b)

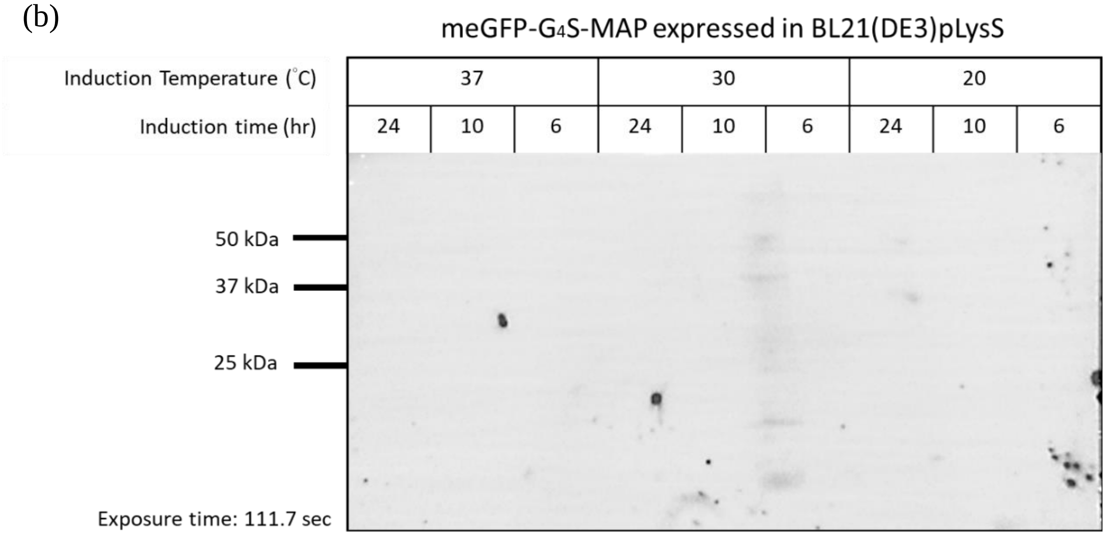

Figure A.3. Duplicate Western blot for expression of meGFP-G4S-MAP (33 kDa) in (a) BL21(DE3), (b) BL21(DE3)pLysS.

Bibliography

1. Centers for Disease Control and Prevention. (2020, May 18). Antimicrobial resistance in *Candida*. Centers for Disease Control and Prevention. https://www.cdc.gov/fungal/diseases/candidiasis/antifungal-resistant.html
2. Govindarajan, A. (2023, May 23). Fluconazole. StatPearls [Internet]. https://www.ncbi.nlm.nih.gov/books/NBK537158/#:~:text=It%20is%20an%20FDA%2Dapproved,%2C%20pneumonia%2C%20and%20cryptococcal%20meningitis.
3. Szymański, M., Chmielewska, S., Czyżewska, U., Malinowska, M., & Tylicki, A. (2022). Echinocandins – structure, mechanism of action, and use in antifungal therapy. Journal of Enzyme Inhibition and Medicinal Chemistry, 37(1), 876–894. https://doi.org/10.1080/14756366.2022.2050224
4. Copolovici, D. M., Langel, K., Eriste, E., & Langel, Ü. (2014). Cell-penetrating peptides: Design, synthesis, and applications. ACS Nano, 8(3), 1972–1994. https://doi.org/10.1021/nn4057269
5. Madani, F., Lindberg, S., Langel, Ü., Futaki, S., & Gräslund, A. (2011). Mechanisms of cellular uptake of cell-penetrating peptides. Journal of Biophysics, 2011, 1–10. https://doi.org/10.1155/2011/414729
6. Uribe-Querol, E., & Rosales, C. (2020). Phagocytosis: Our current understanding of a universal biological process. Frontiers in Immunology, 11. https://doi.org/10.3389/fimmu.2020.01066
7. Terrone, D., Sang, S. L., Roudaia, L., & Silvius, J. R. (2003). Penetratin and related cell-penetrating cationic peptides can translocate across lipid bilayers in the presence of a transbilayer potential. Biochemistry, 42(47), 13787–13799. https://doi.org/10.1021/bi035293y
8. Heitz, F., Morris, M. C., & Divita, G. (2009). Twenty years of cell-penetrating peptides: From molecular mechanisms to therapeutics. British Journal of Pharmacology, 157(2), 195–206. https://doi.org/10.1111/j.1476-5381.2009.00057.x
9. Lee, H.-M., Ren, J., Tran, K. M., Jeon, B.-M., Park, W.-U., Kim, H., Lee, K. E., Oh, Y., Choi, M., Kim, D.-S., & Na, D. (2021). Identification of efficient prokaryotic cell-penetrating peptides with applications in bacterial biotechnology. Communications Biology, 4(1). https://doi.org/10.1038/s42003-021-01726-w
10. Holm, T., Bruchmann, J., Scheynius, A., & Langel. (2011). Cell-penetrating peptides as antifungals towards *Malassezia sympodialis*. Letters in Applied Microbiology, 54(1), 39–44. https://doi.org/10.1111/j.1472-765x.2011.03168.x
11. Gong, Z., & Karlsson, A. J. (2017). Translocation of cell-penetrating peptides into *Candida* fungal pathogens. Protein Science, 26(9), 1714–1725. https://doi.org/10.1002/pro.3203
12. Sudbery, P. E. (2011). Growth of *Candida albicans* hyphae. Nature Reviews Microbiology, 9(10), 737–748. https://doi.org/10.1038/nrmicro2636
13. Cavassin, F. B., Baú-Carneiro, J. L., Vilas-Boas, R. R., & Queiroz-Telles, F. (2021). Sixty Years of Amphotericin B: An overview of the main antifungal agent used to treat invasive fungal infections. Infectious Diseases and Therapy, 10(1), 115–147. https://doi.org/10.1007/s40121-020-00382-7

14. Ruiz-Baca, E., Isela Arredondo-Sánchez, R., Corral-Pérez, K., López-Rodríguez, A., Meneses-Morales, I., M. Ayala-García, V., & Lilia Martínez-Rocha, A. (2021). Molecular mechanisms of resistance to antifungals in *Candida albicans*. Advances in Candida Albicans. https://doi.org/10.5772/intechopen.96346
15. de Oliveira Santos, G. C., Vasconcelos, C. C., Lopes, A. J., de Sousa Cartágenes, M. do, Filho, A. K., do Nascimento, F. R., Ramos, R. M., Pires, E. R., de Andrade, M. S., Rocha, F. M., & de Andrade Monteiro, C. (2018). *Candida* infections and therapeutic strategies: Mechanisms of action for traditional and alternative agents. Frontiers in Microbiology, 9. https://doi.org/10.3389/fmicb.2018.01351
16. Sadiq, I. Z., Muhammad, A., Mada, S. B., Ibrahim, B., & Umar, U. A. (2021). Biotherapeutic effect of cell-penetrating peptides against microbial agents: A Review. Tissue Barriers, 10(3). https://doi.org/10.1080/21688370.2021.1995285
17. Yang, N. J., & Hinner, M. J. (2014). Getting across the cell membrane: An overview for small molecules, peptides, and proteins. Site-Specific Protein Labeling, 29–53. https://doi.org/10.1007/978-1-4939-2272-7_3
18. Arrighi, R. B., Ebikeme, C., Jiang, Y., Ranford-Cartwright, L., Barrett, M. P., Langel, U., & Faye, I. (2008). Cell-penetrating peptide TP10 shows broad-spectrum activity against both *Plasmodium falciparum* and *Trypanosoma brucei brucei*. Antimicrobial Agents and Chemotherapy, 52(9), 3414–3417. https://doi.org/10.1128/aac.01450-07
19. Wimley, W. C. (2021). Synthetic molecular evolution of cell penetrating peptides. Methods in Molecular Biology, 73–89. https://doi.org/10.1007/978-1-0716-1752-6_5
20. Zaro, J. L., & Shen, W.-C. (2015). Cationic and amphipathic cell-penetrating peptides (CPPS): Their structures and in vivo studies in drug delivery. Frontiers of Chemical Science and Engineering, 9(4), 407–427. https://doi.org/10.1007/s11705-015-1538-y
21. Li, Z., Zhang, Y., Zhu, D., Li, S., Yu, X., Zhao, Y., Ouyang, X., Xie, Z., & Li, L. (2017). Transporting carriers for intracellular targeting delivery via non-endocytic uptake pathways. Drug Delivery, 24(2), 45–55. https://doi.org/10.1080/10717544.2017.1391889
22. Van Westering, T., Betts, C., & Wood, M. (2015). Current understanding of molecular pathology and treatment of cardiomyopathy in Duchenne muscular dystrophy. Molecules, 20(5), 8823–8855. https://doi.org/10.3390/molecules20058823
23. Adhikari, S., Alahmadi, T. I., Gong, Z., & Karlsson, A. J. (2018a). Expression of cell-penetrating peptides fused to protein cargo. Microbial Physiology, 28(4), 159–168. https://doi.org/10.1159/000494084
24. Gong, Z., Walls, M. T., Karley, A. N., & Karlsson, A. J. (2016a). Effect of a flexible linker on recombinant expression of cell-penetrating peptide fusion proteins and their translocation into fungal cells. Molecular Biotechnology, 58(12), 838–849. https://doi.org/10.1007/s12033-016-9983-5
25. Jain, A., Shah, S. G., & Chugh, A. (2014). Cell penetrating peptides as efficient nanocarriers for delivery of antifungal compound, natamycin for the treatment of

fungal keratitis. Pharmaceutical Research, 32(6), 1920–1930. https://doi.org/10.1007/s11095-014-1586-x
26. Trofimenko, E., Grasso, G., Heulot, M., Chevalier, N., Deriu, M. A., Dubuis, G., Arribat, Y., Serulla, M., Michel, S., Vantomme, G., Ory, F., Dam, L. C., Puyal, J., Amati, F., Lüthi, A., Danani, A., & Widmann, C. (2021). Genetic, cellular, and structural characterization of the membrane potential-dependent cell-penetrating peptide translocation pore. eLife, 10. https://doi.org/10.7554/elife.69832
27. Royant, A., & Noirclerc-Savoye, M. (2011, April 27). PDB entry - 2Y0G. wwPDB: 2Y0G. https://doi.org/10.2210/pdb2Y0G/pdb
28. Ormö, M., Cubitt, A. B., Kallio, K., Gross, L. A., Tsien, R. Y., & Remington, S. J. (1996). Crystal structure of the aequorea victoria green fluorescent protein. Science, 273(5280), 1392–1395. https://doi.org/10.1126/science.273.5280.1392
29. Kong, J., Wang, Y., Qi, W., Huang, M., Su, R., & He, Z. (2020). Green fluorescent protein inspired fluorophores. Advances in Colloid and Interface Science, 285, 102286. https://doi.org/10.1016/j.cis.2020.102286
30. Cambré, A., & Aertsen, A. (2020). Bacterial vivisection: How fluorescence-based imaging techniques shed a light on the inner workings of bacteria. Microbiology and Molecular Biology Reviews, 84(4). https://doi.org/10.1128/mmbr.00008-20
31. Dunsing, V., Luckner, M., Zühlke, B., Petazzi, R. A., Herrmann, A., & Chiantia, S. (2018). Optimal fluorescent protein tags for quantifying protein oligomerization in living cells. Scientific Reports, 8(1). https://doi.org/10.1038/s41598-018-28858-0
32. Steiner, V., Schär, M., Börnsen, K. O., & Mutter, M. (1991). Retention behaviour of a template-assembled synthetic protein and its amphiphilic building blocks on reversed-phase columns. Journal of Chromatography A, 586(1), 43–50. https://doi.org/10.1016/0021-9673(91)80023-a
33. Silva, S., Kurrikoff, K., Langel, Ü., Almeida, A. J., & Vale, N. (2022). A second life for map, a model amphipathic peptide. International Journal of Molecular Sciences, 23(15), 8322. https://doi.org/10.3390/ijms23158322
34. Oehlke, J., Scheller, A., Wiesner, B., Krause, E., Beyermann, M., Klauschenz, E., Melzig, M., & Bienert, M. (1998). Cellular uptake of an α-helical amphipathic model peptide with the potential to deliver polar compounds into the cell interior non-endocytically. Biochimica et Biophysica Acta (BBA) - Biomembranes, 1414(1–2), 127–139. https://doi.org/10.1016/s0005-2736(98)00161-8
35. Morris, M. C., Deshayes, S., Heitz, F., & Divita, G. (2008). Cell-penetrating peptides: From molecular mechanisms to therapeutics. Biology of the Cell, 100(4), 201–217. https://doi.org/10.1042/bc20070116
36. Simeoni, F. (2003). Insight into the mechanism of the peptide-based Gene Delivery System MPG: Implications for delivery of Sirna into mammalian cells. Nucleic Acids Research, 31(11), 2717–2724. https://doi.org/10.1093/nar/gkg385
37. Elmquist, A., Hansen, M., & Langel, Ü. (2006). Structure–activity relationship study of the cell-penetrating peptide pvec. Biochimica et Biophysica Acta (BBA) - Biomembranes, 1758(6), 721–729. https://doi.org/10.1016/j.bbamem.2006.05.013

38. Elmquist, A., Lindgren, M., Bartfai, T., & Langel, Ü. (2001). VE-cadherin-derived cell-penetrating peptide, pvec, with carrier functions. Experimental Cell Research, 269(2), 237–244. https://doi.org/10.1006/excr.2001.5316
39. Lalatsa, A., Schatzlein, A. G., & Uchegbu, I. F. (2014). Strategies to deliver peptide drugs to the brain. Molecular Pharmaceutics, 11(4), 1081–1093. https://doi.org/10.1021/mp400680d
40. de Oliveira, E. C., da Costa, K. S., Taube, P. S., Lima, A. H., & Junior, C. de. (2022). Biological membrane-penetrating peptides: Computational prediction and applications. Frontiers in Cellular and Infection Microbiology, 12. https://doi.org/10.3389/fcimb.2022.838259
41. Kimple, M. E., & Sondek, J. (2004). Overview of affinity tags for protein purification. Current Protocols in Protein Science, 36(1). https://doi.org/10.1002/0471140864.ps0909s36
42. Köppl, C., Lingg, N., Fischer, A., Krös, C., Loibl, J., Buchinger, W., Schneider, R., Jungbauer, A., Striedner, G., & Cserjan-Puschmann, M. (2022). Fusion tag design influences soluble recombinant protein production in escherichia coli. International Journal of Molecular Sciences, 23(14), 7678. https://doi.org/10.3390/ijms23147678
43. Markmeyer, P., Rühlmann, A., Englisch, U., & Cramer, F. (1990). The PAX plasmids: New gene-fusion vectors for sequencing, mutagenesis and expression of proteins in *escherichia coli*. Gene, 93(1), 129–134. https://doi.org/10.1016/0378-1119(90)90146-i
44. Brown, M. A., Stenberg, L. M., & Stenflo, J. (2013). Coagulation factor xa. Handbook of Proteolytic Enzymes, 2908–2915. https://doi.org/10.1016/b978-0-12-382219-2.00642-6
45. Healey, R. D., Couillaud, L., Hoh, F., Mouhand, A., Fouillen, A., Couvineau, P., Granier, S., & Leyrat, C. (2023). Structure, dynamics and transferability of the metal-dependent polyhistidine tetramerization motif TetrHis for single-chain FV antibodies. Communications Chemistry, 6(1). https://doi.org/10.1038/s42004-023-00962-x
46. Houšť, J., Spížek, J., & Havlíček, V. (2020). Antifungal drugs. Metabolites, 10(3), 106. https://doi.org/10.3390/metabo10030106
47. Mierendorf, R. C., Morris, B. B., Hammer, B., & Novy, R. E. (1998). Expression and purification of recombinant proteins using the pet system. Molecular Diagnosis of Infectious Diseases, 257–292. https://doi.org/10.1385/0-89603-485-2:257
48. Bottens, R. A., & Yamada, T. (2022). Cell-penetrating peptides (CPPS) as therapeutic and diagnostic agents for cancer. Cancers, 14(22), 5546. https://doi.org/10.3390/cancers14225546
49. Nallamsetty, S., Austin, B. P., Penrose, K. J., & Waugh, D. S. (2005). Gateway vectors for the production of combinatorially-tagged his6-mbp fusion proteins in the cytoplasm and periplasm of escherichia coli. Protein Science, 14(12), 2964–2971. https://doi.org/10.1110/ps.051718605
50. Marini, G., Luchese, M. D., Argondizzo, A. P., de Góes, A. C., Galler, R., Alves, T. L., Medeiros, M. A., & Larentis, A. L. (2014). Experimental design approach in recombinant protein expression: Determining medium composition and

induction conditions for expression of pneumolysin from streptococcus pneumoniae in escherichia COLIAND preliminary purification process. BMC Biotechnology, 14(1). https://doi.org/10.1186/1472-6750-14-1

51. Haas, A. K., Maisel, D., Adelmann, J., von Schwerin, C., Kahnt, I., & Brinkmann, U. (2012). Human-protein-derived peptides for intracellular delivery of biomolecules. Biochemical Journal, 442(3), 583–593. https://doi.org/10.1042/bj20111973
52. Ruseska, I., & Zimmer, A. (2020). Internalization mechanisms of cell-penetrating peptides. Beilstein Journal of Nanotechnology, 11, 101–123. https://doi.org/10.3762/bjnano.11.10
53. Quinn, S. E., Huang, L., Kerkvliet, J. G., Swanson, J. A., Smith, S., Hoppe, A. D., Anderson, R. B., Thiex, N. W., & Scott, B. L. (2021). The structural dynamics of macropinosome formation and pi3-kinase-mediated sealing revealed by Lattice Light Sheet Microscopy. Nature Communications, 12(1). https://doi.org/10.1038/s41467-021-25187-1
54. Rosales, C., & Uribe-Querol, E. (2017). Phagocytosis: A fundamental process in immunity. BioMed Research International, 2017, 1–18. https://doi.org/10.1155/2017/9042851
55. Kaksonen, M., & Roux, A. (2018). Mechanisms of clathrin-mediated endocytosis. Nature Reviews Molecular Cell Biology, 19(5), 313–326. https://doi.org/10.1038/nrm.2017.132
56. Kiss, A. L., & Botos, E. (2009). Endocytosis via caveolae: Alternative pathway with distinct cellular compartments to avoid lysosomal degradation? Journal of Cellular and Molecular Medicine, 13(7), 1228–1237. https://doi.org/10.1111/j.1582-4934.2009.00754.x
57. Sarko, D., Beijer, B., Garcia Boy, R., Nothelfer, E.-M., Leotta, K., Eisenhut, M., Altmann, A., Haberkorn, U., & Mier, W. (2010). The pharmacokinetics of cell-penetrating peptides. Molecular Pharmaceutics, 7(6), 2224–2231. https://doi.org/10.1021/mp100223d
58. National Center for Biotechnology Information (2024). PubChem Compound Summary for CID 3365, Fluconazole. Retrieved August 7, 2024 from https://pubchem.ncbi.nlm.nih.gov/compound/Fluconazole.
59. National Center for Biotechnology Information (2024). PubChem Compound Summary for CID 166548, Anidulafungin. Retrieved August 7, 2024 from https://pubchem.ncbi.nlm.nih.gov/compound/Anidulafungin.
60. National Center for Biotechnology Information (2024). PubChem Compound Summary for CID 5280965, Amphotericin B. Retrieved August 7, 2024 from https://pubchem.ncbi.nlm.nih.gov/compound/Amphotericin-B.